Intra-strain elicitation and suppression of plant immunity by *Ralstonia solanacearum* type-III effectors in *Nicotiana benthamiana*

Yuying Sang[1,#], Wenjia Yu[1,2,#], Haiyan Zhuang[1], Yali Wei[1,2], Lida Derevnina[3], Gang Yu[1], Jiamin Luo[1,2] and Alberto P. Macho[1] *.

[1]Shanghai Center for Plant Stress Biology, CAS Center for Excellence in Molecular Plant Sciences; Shanghai Institutes of Biological Sciences, Chinese Academy of Sciences, Shanghai 201602, China.

[2]University of Chinese Academy of Sciences, Beijing, China.

[3]The Sainsbury Laboratory, University of East Anglia, Norwich Research Park, Norwich, NR4 7UH, United Kingdom.

[#] These authors contributed equally to this work, and are mentioned in alphabetical order.

* Corresponding author: Alberto P. Macho, alberto.macho@sibs.ac.cn

Keywords: cell death; ETI; SGT1; effector; immunity; virulence; Ralstonia; salicylic acid; jasmonic acid; ICS1; PAL

Abstract

Effector proteins delivered inside plant cells are powerful weapons for bacterial pathogens, but this exposes the pathogen to potential recognition by the plant immune system. Therefore, the effector repertoire of a given pathogen must be balanced for a successful infection. *Ralstonia solanacearum* is an aggressive pathogen with a large repertoire of secreted effectors. One of these effectors, RipE1, is conserved in most *R. solanacearum* strains sequenced to date. In this work, we found that RipE1 triggers immunity in *N. benthamiana*, which requires the immune regulator SGT1, but not EDS1 or NRCs. Interestingly, RipE1-triggered immunity induces the accumulation of salicylic acid (SA) and the overexpression of several genes encoding phenylalanine-ammonia lyases (PALs), suggesting that the unconventional PAL-mediated pathway is responsible for the observed SA biosynthesis. Surprisingly, RipE1 recognition also induces the expression of jasmonic acid (JA)-responsive genes and JA biosynthesis, suggesting that both SA and JA may act cooperatively in response to RipE1. Finally, we found that RipE1 expression leads to the accumulation of glutathione in plant cells, which precedes the activation of immune responses. *R. solanacearum* encodes another effector, RipAY, which is known to inhibit immune responses by degrading cellular glutathione. Accordingly, we show that RipAY inhibits RipE1-triggered immune responses. This work shows a strategy employed by *R. solanacearum* to counteract the perception of its effector proteins by the plant immune system.

Introduction

Ralstonia solanacearum is considered one of the most destructive plant pathogens, and is able to cause disease in more than 250 plant species (Jiang et al., 2017; Mansfield et al., 2012). As a soil-borne bacterial pathogen, *R. solanacearum* enters plants through the roots, reaches the vascular system, and spreads through xylem vessels, colonizing the plant systemically (Mansfield et al., 2012). This is followed by massive bacterial replication and the disruption of the plant vascular system, leading to eventual plant wilting (Digonnet et al., 2012; Turner et al., 2009).

Most bacterial pathogens deliver proteins inside plant cells via a type-III secretion system (T3SS); such proteins are thus called type-III effectors (T3Es) (Galan et al, 2014). T3Es have been reported to mediate the suppression of basal defenses and the manipulation of plant physiological functions to support bacterial proliferation (Macho et al, 2015; Macho, 2016). Resistant plants have evolved intracellular receptors defined by the presence of nucleotide-binding sites (NBS) and leucine-rich repeat domains (LRRs), thus termed NLRs (Cui et al, 2015). Specific NLRs can detect the activities of specific T3Es, leading to the activation of immune responses, which effectively prevent pathogen proliferation (Chiang & Coaker, 2015). The outcome of these responses is named effector-triggered immunity (ETI), and, in certain cases, may cause a hypersensitive response (HR) that involves the collapse of plant cells. Hormone-mediated signaling plays an essential role in plant immunity. Salicylic acid (SA) is considered the most important hormone in plant immunity against biotrophic pathogens (Vlot *et al.*, 2009; Burger & Chory, 2019); Jasmonic acid (JA), on the other hand, is considered the main mediator of immune responses against necrotrophic pathogens (Burger & Chory, 2019). In most cases, both hormones are considered as antagonistic, balancing the effects of each other (Burger & Chory, 2019).

In an evolutionary response to ETI, successful pathogens have acquired T3E activities to suppress this phenomenon (Jones & Dangl, 2006), although reports

73 characterizing T3E suppression of ETI remain scarce, particularly among T3Es within
74 the same strain. While the development of additional T3E activities is a powerful
75 virulence strategy, it also exposes the pathogen to further events of effector
76 recognition. Therefore, the benefits and penalties of T3E secretion need to be finely
77 and dynamically balanced in specific hosts, to ensure the appropriate manipulation of
78 plant functions while evading or suppressing ETI. This balance may be particularly
79 important for *R. solanacearum*, which secretes a larger number of T3Es in
80 comparison to other bacterial plant pathogens (*e.g.* the reference GMI1000 strain is
81 able to secrete more than 70 T3Es) (Peeters et al, 2013).
82
83 Plants have evolved to recognize immune elicitors from *R. solanacearum* (Wei et al,
84 2018; Jayaraman et al., 2016). In terms of mechanism of T3E recognition, the most
85 studied case in *R. solanacearum* is RipP2 (also known as PopP2), which is perceived
86 in Arabidopsis by the RRS1-RPS4 NLR pair (Gassmann et al, 1999; Deslandes et al,
87 2002; Tasset et al, 2010; Williams et al, 2014; Le Roux et al, 2015; Sarris et al, 2015).
88 Additionally, several *R. solanacearum* T3Es were shown to induce cell death in
89 different plant species (Peeters et al, 2013; Clarke et al, 2015), although, in most
90 cases, it is unclear whether these are due to toxic effects caused by effector
91 overexpression or a host immune response. Some *R. solanacearum* T3Es have also
92 been shown to cause a restriction of host range; such is the case for RipAA and
93 RipP1 (also known as AvrA and PopP1, respectively), which are perceived and
94 restrict host range in *Nicotiana* species (Poueymiro et al, 2009). RipP1 also triggers
95 resistance in petunia (Lavie et al, 2002). Similarly, RipB-triggered immunity has been
96 reported as the major cause for avirulence of *R. solanacearum* RS1000 in *Nicotiana*
97 species (Nakano & Mukaihara, 2019), RipAX2 (also known as Rip36) have been
98 shown to induce resistance in eggplant and its wild relative *Solanum torvum* (Nahar et
99 al, 2014; Morel et al, 2018a), and several T3Es from the AWR family (also known as
100 RipA) restrict bacterial growth in Arabidopsis (Sole et al, 2012). Although the
101 utilization of these recognition systems to generate disease-resistant crops is
102 tantalizing, it is imperative to understand the mechanisms underlying the activation of

103 plant immunity and their potential suppression by other T3Es within *R. solanacearum*.

104

105 The *ripE1* gene encodes a protein secreted by the type-III secretion system in the *R.*
106 *solanacearum* GMI1000 strain (phylotype I) (Mukaihara et al, 2010), and is conserved
107 across *R. solanacearum* strains from different phylotypes (Peeters et al, 2013). Based
108 on sequence analysis, RipE1 is homologous to other T3Es in *Pseudomonas syringae*
109 (HopX) and *Xanthomonas spp* (XopE) (Figure S1; Peeters et al, 2013), belonging to
110 the HopX/AvrPphB T3E family (Nimchuk et al, 2007). This family is characterized by
111 the presence of a putative catalytic triad consisting of specific cysteine, histidine, and
112 aspartic acid residues, which are conserved in RipE1 (Nimchuk et al, 2007; Figure
113 S1), and is similar to several enzyme families from the transglutaminase protein
114 superfamily, such as peptide N-glycanases, phytochelatin synthases, and cysteine
115 proteases (Makarova et al, 1999). AvrPphB, from *P. syringae* pv. *phaseolicola*, the
116 original member of the HopX/AvrPphB family, was identified based on its ability to
117 activate immunity in certain bean cultivars (Mansfield et al, 1994). Divergent members
118 from this family in other strains also trigger immunity, and this requires the putative
119 catalytic cysteine (Nimchuk et al, 2007). Previous sequence analysis of T3Es from the
120 HopX family also identified a conserved domain (domain A) required for HopX
121 induction of immunity in bean and Arabidopsis, which as hypothesized to represent a
122 host-target interaction domain or a novel nucleotide/cofactor binding domain
123 (Nimchuk et al, 2007).

124

125 In this work, we studied the impact of RipE1 in plant cells, and found that RipE1 is
126 recognized by the plant immune system in both *N. benthamiana* and Arabidopsis,
127 leading to the activation of immune responses. We further investigate the immune
128 components and signaling pathways associated to this effector recognition. Finally,
129 we found that another effector in *R. solanacearum* GMI1000 is able to inhibit
130 RipE1-triggered immune responses in *N. benthamiana*, explaining the fact that RipE1
131 does not seem to be an avirulence determinant in this plant species.

132 **Results**

133

134 **RipE1 triggers cell death upon transient expression in *Nicotiana benthamiana***

135

136 In order to understand the impact of RipE1 in plant cells, we first used an
137 *Agrobacterium tumefaciens* (hereafter, Agrobacterium)-mediated expression system
138 in *Nicotiana benthamiana* leaves to transiently express RipE1 that is fused to a
139 carboxyl-terminal green fluorescent protein (GFP) tag (RipE1-GFP). Two days after
140 Agrobacterium infiltration, we noticed the collapse of infiltrated tissues expressing
141 RipE1-GFP, but not a GFP control (Figure 1a). This tissue collapse correlated with a
142 release of ions from plant cells (Figure 1b), and cell death was confirmed by trypan
143 blue staining (Figure S2). Mutation of the catalytic cysteine to an alanine residue has
144 been shown to disrupt the catalytic activity of enzymes with a catalytic triad similar to
145 that conserved in RipE1 (Gimenez-Ibanez et al, 2014; Figure 1c). To determine if the
146 putative catalytic activity is required for RipE1 induction of cell death, we generated an
147 equivalent mutant in RipE1 (C172A; Figure 1c). We also generated an independent
148 mutant with a deletion on the eight amino acids that constitute the conserved domain
149 A (Nimchuk et al, 2007; Figure 1c). These mutations did not affect the accumulation of
150 RipE1 (Figure 1d), but abolished the induction of tissue collapse and the ion leakage
151 caused by RipE1 expression (Figure 1e and 1f), indicating that RipE1 requires both
152 the catalytic cysteine and the conserved domain A for the induction of cell death in
153 plants.

154

155 Interestingly, RipE1 was also identified in a systematic screen performed in our
156 laboratory to identify *R. solanacearum* T3Es that suppress immune responses
157 triggered by bacterial elicitors. In this screen we found that RipE1 expression
158 suppresses the burst of reactive oxygen species (ROS) and the activation of
159 mitogen-activated protein kinases (MAPKs) triggered upon treatment with the
160 bacterial flagellin epitope flg22, which acts as an immune elicitor (Figure S3a and
161 S3b). RipE1 requires both the catalytic cysteine and the conserved domain A for this

162 activity (Figure S3c). However, we considered the possibility that these responses are
163 abolished by the death of plant cells rather than an active immune suppression.
164 Time-course experiments showed that the suppression of flg22-triggered ROS
165 correlated with the appearance of cell death (Figure S3a and S3d), making it difficult
166 to uncouple these observations.
167
168 **RipE1 activates salicylic acid-dependent immunity in *N. benthamiana***
169
170 The induction of cell death by pathogen effectors may reflect toxicity in plant cells or
171 the activation of immune responses that lead to a HR. Salicylic Acid (SA) plays a
172 major role in the activation of immune responses after the perception of different types
173 of invasion patterns (Vlot *et al.*, 2009). To determine whether RipE1 activates immune
174 responses, we first measured the expression of the *N. benthamiana* ortholog of the
175 Arabidopsis gene *PATHOGENESIS-RELATED-1* (*PR1*), which is a hallmark of
176 SA-dependent immune responses (Vlot et al., 2009, Ward *et al.*, 1991). Expression of
177 RipE1-GFP (but not the C172A catalytic mutant) significantly enhanced the
178 accumulation of *NbPR1* transcripts (Figure 2a). In keeping with the notion that RipE1
179 activates a defense response against *R. solanacearum*, RipE1 expression in *N.*
180 *benthamiana* leaves enhanced resistance against subsequently inoculated *R.*
181 *solanacearum* Y45, which is otherwise pathogenic in *N. benthamiana* (Li *et al.*, 2011)
182 (Figure 2b). The bacterial salicylate hydroxylase NahG converts SA to catechol, which
183 leads to the suppression of SA-dependent responses (Delaney et al., 1994). The
184 expression of NahG-GFP in *N. benthamiana* slightly enhanced the accumulation of
185 RipE1 fused to a carboxyl-terminal N-luciferase tag (Nluc) (Figure S4), consistent with
186 the reported role of SA in hindering Agrobacterium-mediated transformation
187 (Rosas-Diaz et al, 2016); despite this, *NahG* expression partially suppressed
188 RipE1-triggered cell death, ion leakage, and *NbPR1* expression (Figure 2c, d and e).
189 Altogether, these data suggest that RipE1 induces SA-dependent immune responses
190 in plant cells, which cause the development of a HR.
191

192 **RipE1 enhances the expression of *PAL* genes and the biosynthesis of salicylic**
193 **acid and jasmonic acid**
194
195 The expression of RipE1 led to a dramatic increase in SA accumulation in *N.*
196 *benthamiana* (Figure 3a), consistent with the observed overexpression of *NbPR1*
197 (Figure 2a). This reinforces the idea that RipE1 is perceived by the plant immune
198 system and this leads to the activation of SA biosynthesis and SA-dependent immune
199 responses. In Arabidopsis, the chloroplastic pathway mediated by isochorismate
200 synthethase 1 (ICS1) plays a predominant role in the pathogen-induced SA
201 biosynthesis (Wildermuth et al, Nature, 2001; Garcion et al, Plant Physiology, 2008).
202 However, gene expression analysis showed that the expression of the *N.*
203 *benthamiana* ortholog of the Arabidopsis *ICS1*, *NbICS1*, was significantly reduced
204 upon RipE1 expression (Figure 3b), despite the simultaneous high *NbPR1* transcript
205 accumulation (Figure 2a). SA can also be synthesized from phenylalanine in a
206 pathway mediated by phenylalanine ammonia lyases (PALs). In contrast with the
207 expression of *NbICS1*, several genes encoding NbPALs were up-regulated upon
208 expression of RipE1, but not the catalytic mutant version (Figure 3c-e), suggesting
209 that this pathway may mediate the enhancement of SA biosynthesis upon perception
210 of RipE1 activity. SA and Jasmonic Acid (JA) are considered antagonistic hormones
211 in plant immune responses. Surprisingly, instead of a reduction of JA-associated gene
212 expression, we found a slight increase in the accumulation of *NbLOX2* transcripts in
213 early time points upon expression of catalytically active RipE1 (Figure 3f). In
214 Arabidopsis, LOX2 contributes to the biosynthesis of JA (Bell et al, 1995). Accordingly,
215 we detected an increase in JA contents upon RipE1 expression (Figure S5), indicating
216 that RipE1 perception does not inhibit JA signalling, but rather leads to an
217 enhancement of JA biosynthesis and associated gene expression.
218
219 **RipE1-triggered immunity requires SGT1, but not EDS1 or NRC proteins**
220
221 The suppressor of the G2 allele of *skp1* (SGT1) plays an essential role in ETI, and is

222 required for the induction of disease resistance mediated by most NLRs (Azevedo *et*
223 *al.*, 2002; Kadota *et al.*, 2010). Virus-induced gene silencing (VIGS) of *NbSGT1*
224 abolished RipE1-triggered cell death, ion leakage, and *NbPR1* expression (Figure
225 4a-d), indicating that RipE1-triggered immunity requires SGT1. While most NLRs
226 require SGT1 to function, a specific group of NLRs containing an N-terminal Toll-like
227 interleukin-1 receptor (TIR) domain also require EDS1 (Wiermer et al, 2005; Schultink
228 et al, 2017). *N. benthamiana* plants carrying a stable knockout mutation in *EDS1*
229 (Schultink et al, 2017) displayed clear RipE1-triggered cell death (Figure 4e),
230 suggesting that RipE1-triggered immunity is not mediated by a TIR-NLR. Other NLRs
231 contain a C-terminal coiled coil (CC) domain, and a specific subset of CC-NLRs
232 require a network of helper NLRs termed NRC proteins (Wu et al, 2016). Interestingly,
233 silencing of NRC proteins did not impact RipE1-triggered cell death (Figure S6),
234 suggesting that RipE1-triggered immunity is not mediated by an NLR within the NRC
235 network.
236
237 **RipE1 activates immunity in Arabidopsis**
238
239 Arabidopsis transgenic plants expressing RipE1-GFP from a *35S* inducible promoter
240 died after germination (data not shown). Therefore, we generated Arabidopsis
241 transgenic plants expressing RipE1-GFP and RipE1^{C172A}-GFP from an estradiol
242 (EST)-inducible promoter. Five-week-old plants expressing RipE1-GFP, but not
243 RipE1^{C172A}-GFP, showed reduced growth in soil upon EST treatment for 14 days
244 (Figure 5a). To determine whether RipE1-triggered growth reduction in Arabidopsis
245 correlates with the activation of immunity, we first monitored the expression of
246 defence-related genes. Similar to the result observed upon expression in *N.*
247 *benthamiana*, expression of RipE1 in Arabidopsis triggered the overexpression of
248 *AtPR1* (Figure 5b). However, in Arabidopsis, the enhanced *PR1* expression
249 correlated with an overexpression of *AtICS1*, but not *AtPAL1*, upon RipE1 expression
250 (Figure 5b). As observed in *N. benthamiana*, RipE1 expression led to the
251 overexpression of the JA marker genes *AtVSP2* and *AtPDF1*.2 (Figure 5b). This

252 indicates that, as observed in *N. benthamiana*, RipE1 activates SA- and
253 JA-dependent signalling in Arabidopsis. To determine whether the activation of
254 defence-related genes in Arabidopsis leads to an efficient immune response against
255 *R. solanacearum*, we inoculated RipE1-expressing plants by soil-drenching with *R.*
256 *solanacearum* after EST treatment for 2 days. As shown in the figure 5c,
257 RipE1-expressing plants displayed weaker and delayed disease symptoms upon *R.*
258 *solanacearum* inoculation, reflecting an enhanced disease resistance upon *RipE1*
259 expression. RipE1-expressing plants also showed a moderate reduction in bacterial
260 growth after *R. solanacearum* infiltration in the leaves (Figure S7a), suggesting that
261 the immune response is not exclusively associated to invasion or proliferation in the
262 root. However, RipE1-expressing plants did not display enhanced resistance against
263 the leaf-borne pathogen *Pseudomonas syringae* pv. *tomato* DC3000 (Figure S7b and
264 S7c).
265
266 **RipE1-triggered immune responses are suppressed by RipAY**
267
268 RipE1 expression activates immunity in Arabidopsis and *N. benthamiana*, although
269 both plant species are susceptible hosts for *R. solanacearum* GMI1000 (or a
270 derivative strain carrying mutations in *ripP1* and *ripAA*, in the case of *N. benthamiana*;
271 Poueymiro et al, 2009), which carries RipE1. Therefore, we reasoned that other T3E(s)
272 in GMI1000 may be able to suppress RipE1-triggered immunity in the context of
273 infection. We recently identified a *R. solanacearum* T3E, RipAY, which is able to
274 suppress SA-dependent immune responses through the degradation of glutathione
275 (Sang et al, 2016; Mukaihara et al, 2016); however, the ability of RipAY to suppress
276 immunity triggered by other *R. solanacearum* T3Es remained unknown. Interestingly,
277 the expression of RipE1 in *N. benthamiana* leads to an increase in glutathione
278 accumulation in plant tissues, which precedes the onset of immune responses (Figure
279 6a). Considering that both RipAY and RipE1 are present in GMI1000, we sought to
280 determine if RipAY has the ability to suppress RipE1-triggered immunity. Indeed,
281 expression of RipAY in *N. benthamiana* did not affect the accumulation of RipE1

282 (Figure S8), but abolished the tissue collapse and ion leakage caused by *RipE1*
283 expression (Figure 6b and c). Moreover, RipAY was able to suppress the
284 overexpression of several SA-related genes triggered by RipE1 (Figure 6d and S9),
285 indicating that RipAY suppresses RipE1-triggered immune responses. RipAY did not
286 significantly suppress the RipE1-triggered expression of *NbLOX2* (Figure S9),
287 although this may be due to the weaker induction of this gene compared to the tested
288 SA-related genes (Figure 3 and S9). Interestingly, however, a RipAY point mutant
289 unable to degrade glutathione ($RipAY^{E216Q}$; Sang et al, 2016) did not suppress
290 RipE1-triggered responses (Figure 6b-d), suggesting that RipAY suppresses
291 RipE1-triggered immunity through the degradation of cellular glutathione.
292
293

294 **Discussion**

295

296 Expression of T3Es in plant cells may either induce cell death because of cell toxicity
297 or lead to the activation of an immunity-associated HR. Over-expression of RipE1 in *N.*
298 *benthamiana* leads to a HR that: (*i*) is dependent on the immune regulator SGT1; (*ii*)
299 activates SA accumulation and *PR1* expression; (*iii*) restricts growth of *R.*
300 *solanacearum* Y45; and (*iv*) is suppressed by the NahG and other *R. solanacearum*
301 effectors, indicating that RipE1-mediated cell death is due to the activation of
302 immunity in the host. It is, however, noteworthy that cell death induced by RipE1
303 develops slower than that triggered by other HR-inducing T3Es (*i.e.* RipAA; Figure
304 S2). Several T3Es within the HopX/AvrPphB family are predicted enzymes that are
305 associated with activation of host immunity, although the association of the predicted
306 catalytic activity with the activation of immunity seems to be differ among them. While
307 the ability of AvrPphB and several other family members to trigger immunity requires
308 the putative catalytic cysteine (Mansfield et al, 1994; Nimchuk et al, 2007), other
309 members with the predicted catalytic activity, such as HopX from *P. syringae* pv
310 *tabaci* or *P. syringae* pv *phaseolicola* race 6, do not trigger immunity in the same
311 hosts (Stevens et al, 1998; Nimchuk et al, 2007). In the case of RipE1, the putative
312 catalytic cysteine is required for the induction of immunity, which suggests that RipE1
313 is an active enzyme, and that this catalytic activity leads to perception by the host
314 immune system. Moreover, the conserved domain A (Nimchuk et al, 2007) is also
315 required for the activation of immunity by RipE1. In addition, we found that RipE1 is
316 able to suppress elicitor-triggered immune responses in *N. benthamiana*. However,
317 since this activity correlates with the induction of cell death, it is difficult to uncouple
318 both observations, and further studies on the virulence activity of RipE1 will require
319 the utilization of a host plant that is unable to recognize it.

320

321 The fact that RipE1 is recognized, and activate immune responses, in both *N.*
322 *benthamiana* and Arabidopsis suggests at least two scenarios: it is possible that the
323 NLR responsible for this recognition is conserved in both species; on the other hand, it

324 is also possible that both species have independently develop NLRs that recognize
325 RipE1. Although we did not identify the NLR involved, we determined that, at least in
326 *N. benthamiana*, RipE1 recognition does not rely on EDS1 or the NRC network,
327 pointing to a CC- NRC-independent NLR. Interestingly, although RipE1 perception
328 leads to the accumulation of SA in both plant species, the associated gene expression
329 patterns seem to differ. The ICS pathway plays a predominant role in the
330 pathogen-induced SA biosynthesis in Arabidopsis (Wildermuth et al, Nature, 2001;
331 Garcion et al, Plant Physiology, 2008). In agreement with this, the RipE1-triggered
332 overexpression of *AtPR1* in Arabidopsis correlates with an enhanced expression of
333 *AtICS1*, but not *AtPAL1*. However, it seems that the RipE1-induced increase in SA
334 content in *N. benthamiana* correlates with a reduction of *NbICS1* gene expression,
335 and an increase in the expression of several *NbPAL* genes. Considering that ICS1 is
336 normally regulated at the transcriptional level upon pathogen perception (Wildemurth
337 et al, 2001), our results suggest that the PAL pathway is more relevant than the ICS
338 pathway for the induction of RipE1-triggered immunity in *N. benthamiana*, indicating
339 that both pathways are differentially required for distinct immune responses in
340 different plant species. Similarly, both the ICS and PAL pathways have been reported
341 to be required for pathogen-induced SA biosynthesis in soybean (Shine et al, 2016).
342 The reduction in ICS1 expression in *N. benthamiana* may reflect a compensatory
343 effect between the ICS and PAL pathway. In addition to different gene expression
344 patterns, the physiological output in both plant species may be different. Although
345 RipE1 expression caused an inhibition of Arabidopsis growth, we did not observe any
346 signs of cell death (data not shown), which contrasts with our observation in *N.*
347 *benthamiana*. However, this may be caused by differences in the expression system
348 used in both plants (Agrobacterium-mediated transient expression in *N. benthamiana*
349 *vs* EST-induced expression in Arabidopsis stable transgenic plants).
350
351 Another surprising aspect of RipE1-triggered immunity is the fact that it leads to the
352 simultaneous accumulation of SA and JA, and to a strong and moderate SA- and
353 JA-triggered gene expression, respectively, in both *N. benthamiana* and Arabidopsis.

354 This suggests that, in the case of RipE1-triggered immunity, SA and JA may play a
355 cooperative role, possibly reflecting the complexity of the *R. solanacearum* infection
356 process compared to other pathogens. In keeping with this notion, although
357 RipE1-expressing Arabidopsis plants displayed enhanced resistance against *R.*
358 *solanacearum* and up-regulation of SA-related genes, they did not show enhanced
359 resistance against the leaf-borne pathogen *P. syringae pv. tomato* DC3000 (Figure
360 S6). Since the enhancement of JA signalling has been associated to a promotion of
361 virulence by this pathogen (Gimenez-Ibanez *et al*, 2016), the observed up-regulation
362 of JA-related genes may underlie this phenomenon.
363
364 If RipE1 triggers immunity in *N. benthamiana*, why is it that a GMI1000 strain without
365 RipP1 and RipAA (but having RipE1) can cause a successful infection in *N.*
366 *benthamiana* without triggering immunity (Poueymiro et al, 2009)? Here, we found
367 that another effector within GMI1000, RipAY, is able to inhibit RipE1-triggered
368 immunity. Since RipE1 perception correlates with an enhancement of cellular
369 glutathione, and RipAY requires its gamma-glutamyl cyclotransferase activity to inhibit
370 RipE1-triggered HR, the degradation of glutathione or other gamma-glutamyl
371 compounds (Sang et al, 2016; Mukaihara et al, 2016; Fujiwara et al, 2016) is the most
372 likely mechanism for this inhibition. Besides RipAY, other T3Es within GMI1000 likely
373 contribute to the suppression of RipE1-triggered HR by targeting other immune
374 functions (Yu et al, bioRxiv, 2019; Wang & Macho, unpublished data). This reflects
375 bacterial adaptation: RipE1 could be important for virulence, but also triggers
376 immunity. In this context, instead of losing RipE1, *R. solanacearum* has developed
377 other effectors to suppress the induction of immunity, while keeping RipE1 virulence
378 activity. This is reminiscent of what has been shown for *P. syringae* pv. *syringae*
379 B728a, where several effectors within the same strain suppress the HR triggered by
380 HopZ3, which otherwise acts as a virulence factor (Rufian et al, 2018). Similarly,
381 although transient expression of HopX from *P. syringae* pv *tomato* (*Pto*) triggers HR in
382 specific Arabidopsis accessions, it does not trigger HR in the context of *Pto* infection
383 (Nimchuk et al, 2007). It is possible that, as in the case of RipE1, the immune

384 responses triggered by HopX are masked during *Pto* infection (as suggested in
385 Nimchuk et al, 2007), likely due to the suppression by other effectors within the same
386 strain.
387
388

389 **Materials and Methods**

390

391 **Plant materials and growth conditions**

392 *N. benthamiana* plants were grown on soil at one plant per pot in an environmentally
393 controlled growth room at 25 ºC under a 16-h light/8-h dark photoperiod with a
394 light-intensity of 130 mE $m^{-2}s^{-1}$. *A. thaliana* plants were grown under the same
395 conditions as *N. benthamiana* for collection of seeds. For bacterial virulence and ROS
396 burst assays, *A. thaliana* plants were grown in a growth chamber controlled at 22°C
397 with a 10 h photoperiod and a light-intensity of 100-150 mE $m^{-2}s^{-1}$. After *R.*
398 *solanacearum* inoculation, Arabidopsis plants were transferred to a growth chamber
399 at 27°C with 75% humid under a 12-h light/12-h dark photoperiod.

400

401 **Chemicals**

402 The flg22 peptide (TRLSSGLKINSAKDDAAGLQIA) was purchased from Abclonal,
403 USA. All other chemicals were purchased from Sigma-Aldrich unless otherwise
404 stated.

405

406 **Plasmids, bacterial strains and cultivation conditions**

407 *R. solanacearum* GMI1000 was grown on solid BG medium plates or cultivated
408 over-night in liquid BG medium at 28°C (Morel et al., 2018b). The *ripE1* gene from *R.*
409 *solanacearum* GMI1000 cloned in pDONR207 (donated by Nemo Peeters and
410 Anne-Claire Cazale) was subcloned into pGWB505 by LR reaction (ThermoFisher,
411 USA) to generate a fusion protein with eGFP tag at the C-terminal (Nakagawa *et al.*,
412 2007). *RipE1* and *ripE1* mutants were inserted between BamHI and XhoI restriction
413 sites on sXVE:GFPc:Bar estradiol inducible vector using enzyme digestion
414 (Schlücking et al., 2013). These generated binary vectors were transformed into
415 *Agrobacterium tumefaciens* (Agrobacterium) GV3101 *f*or transient or stable gene
416 expression in *N. benthamiana* and *A. thaliana* plants. Agrobacterium carrying
417 pGWB505 vectors were grown at 28°C and 220 rpm in LB medium supplemented with
418 rifampicin 50 mg/l, gentamycin 25 mg/l and spectinomycin 50 mg/l, while those

419 carrying estradiol inducible vectors were grown in rifampicin 50 mg/l, gentamycin 25
420 mg/l and kanamycin 50 mg/l.
421
422 **Site-directed mutagenesis**
423 *RipE1*$_{C172A}$ and *RipE1 ΔAD* mutant variants were generated using the QuickChange
424 Lightning Site-Directed Mutagenesis Kit (Life technologies, USA) following the
425 manufacturer's instructions. RipE1/pDONR207 plasmid was used as template.
426 Primers used for the mutagenesis are listed in Table S1.
427
428 **Agrobacterium-mediated gene expression in *A. thaliana and N. benthamiana***
429 Stable transgenic Arabidopsis plants with *RipE1* and *RipE1* mutated variants driven
430 by estradiol inducible promoter were obtained using the floral dip method (Zhang et. al,
431 2006). Homozygous T_3 lines were used for all the experiments.
432 Agrobacterium-mediated transient expression in *N. benthamiana* was performed as
433 described (Li, 2011). Agrobacterium carrying the resultant plasmids were suspended
434 in infiltration buffer to a final OD_{600} of 0.1~0.5 and infiltrated into the abaxial side of the
435 leaves using the 1 ml needless syringe. Leaf samples were taken at 1-3 dpi (days
436 post infiltration) for analysis based on experimental requirements.
437
438 **Protein extraction and western blots**
439 Plant tissues were collected into 2 ml tubes with metal beads and frozen in liquid
440 nitrogen. After grinding with a tissue lyser (Qiagen, Germany) for 1 min at 30 rpm/s,
441 proteins were extracted using protein extraction buffer (100 mM Tris-HCl pH 8, 150
442 mM NaCl, 10% glycerol, 5 mM Ethylene diamine tetra acetic acid (EDTA), 2 mM
443 Dithiothreitol (DTT), 1x Plant Protease Inhibitor cocktail, 1% NP-40, 2 mM
444 Phenylmethylsulfonyl fluoride (PMSF), 10 mM Na_2MoO_4, 10 mM NaF, 2 mM Na_3VO_4)
445 and incubating for 5 min. After centrifugation, the supernatants were mixed with SDS
446 loading buffer, incubated at 70 ºC for 10 min, and resolved using SDS-PAGE.
447 Proteins were transferred to a PVDF membrane and monitored by western blot using
448 anti-GFP (Abicode, M0802-3a) and anti-luciferase (Sigma, L0159) antibodies.

449

450 **Measurement of ROS generation and MAPK activation**

451 PAMP-triggered ROS burst and MAPK activation in plant leaves were measured as
452 described previously (Sang et al., 2017; Segonzac *et al.*, 2011). ROS was elicited with
453 50 nM flg22. MAPK activation assays were performed using 4 to 5-week-old *N.*
454 *benthamiana*. Two days after Agrobacterium infiltration at OD_{600} of 0.1, the intact
455 leaves were elicited for 15 min after vacuum infiltration of 100 nM flg22. Leaf discs
456 were taken to monitor MAPK activation by western blot with Phospho-p44/42 MAPK
457 (Erk1/2; Thr-202/Tyr-204) antibodies.

458

459 **Cell death measurement**

460 Cell death in plant leaves was quantified as previously described (Yu et al, bioRxiv,
461 2019) by measuring the electrolyte leakage using a conductivity meter (ThermoFisher,
462 USA) or observing the autofluorescence using the BioRad Gel Imager (Bio-Rad, USA).
463 Briefly, one day after Agrobacterium infiltration in *N. benthamiana*, one 13 mm leaf
464 disk was immersed in 4 ml of distilled water for 1 h with gentle shaking and then
465 transferred to a 6-well culture plate containing 4 ml distilled water in each well. The ion
466 conductivity was then measured at different time intervals. Autofluorescence in intact
467 *N. benthamiana* leaves was measured at 2.5 dpi. Trypan blue staining was performed
468 as previously described (Lv *et al*, 2019).

469

470 **RNA isolation and qRT-PCR**

471 Five-to-eight day-old Arabidopsis seedlings were grown in sterile conditions and 8-10
472 seedlings grown in an independent plate were collected as one biological sample.
473 Total RNA was extracted using the E.Z.N.A. Plant RNA kit with DNA digestion on
474 column (Biotek, China) according to the manufacturer's instructions. RNA samples
475 were quantified with a Nanodrop spectrophotometer (ThermoFisher, USA). First
476 strand cDNA was synthesized using the iScript^{TM} cDNA synthesis kit (Bio-Rad).
477 qRT-PCR was performed using the iTaq^{TM} Universal SYBR Green Supermix (Bio-Rad)
478 and CFX96 Real-time system (Bio-Rad) and the qPCR data was analyzed as

479 previously described (Livak & Schmittgen, 2001; Wang et al, 2019). Primers for qPCR
480 of SA-JA related genes in *N. benthamiana* were used as described by Nakano and
481 Mukaihara (2018). Primer sequences are listed in Table S1.
482
483 **Measurements of SA and JA content in plant leaves**
484 SA and JA content were quantified using the method described by Forcat and
485 collaborators (2008) with the following modifications. Leaves (50 mg FW) were
486 collected 42 hours after Agrobacterium infiltration and frozen in liquid nitrogen before
487 grounding into fine powder with the Qiagen tissue lyser. SA and JA were extracted at
488 10 ∘ C for 1 h using 70% methanol extraction solvent spiked with d4-SA as internal
489 standards. Supernatant was taken after centrifugation at 20000 rcf for 10 min and
490 analyzed on ACQUITY UPLC I-class coupled with AB SCIEX TripleTOF 5600+. The
491 analytical column used was a ACQUITY UPLC BECH C18 1.7 μm, 2.1X150 mm
492 column. The JA concentration was calculated based on the calibration curve created
493 by running a JA standard solution. The results were analyzed by Peakview1.2.
494
495 **Measurements of total cellular glutathione in *N. benthamiana* leaves**
496 Total cellular glutathione was measured as previously described (Sang et al, 2016).
497 Briefly, 10 mg of *N. benthamiana* leaves were collected and glutathione was
498 measured using a Glutathione Assay Kit (Beyotime, China) according to the
499 manufacturer's instructions.
500
501 **Virus-induced gene silencing (VIGS) in *N. benthamiana***
502 VIGS in *N. benthamiana* plants was performed using TRV vectors as described
503 (Senthil-Kumar & Mysore, 2014). VIGS of *NbSGT1* was performed with several
504 modifications described by Yu and collaborators (2019). Cultures of Agrobacterium
505 carrying pTRV2:*NbSGT1* plasmids or pTRV2 plasmids were mixed at 1:1 ratio and
506 co-infiltrated into the lower leaves of 3-week-old *N. benthamiana* plants. The upper
507 leaves were used for experimental assay within 7-10 days after VIGS application.
508 Silencing of NRCs (NLR required for cell death) in *N. benthamiana* and subsequent

509 expression of T3Es was performed as described by Wu and collaborators (2017).

510

511 ***Pseudomonas syringae* virulence assays**

512 For leaf infiltration with *P. syringae*, Arabidopsis plants were treated with 100 µM EST
513 for 2 days before inoculation. Plants showed no difference in root or shoot size at the
514 time of inoculation. *Pto* DC3000 was resuspended in water at 10^5 cfu/ml. The bacterial
515 suspensions were then infiltrated into 4-to-5-week-old Arabidopsis leaves using a
516 needleless syringe. For spray inoculation, *Pto* DC3000 was resuspended in water at
517 10^8 cfu/ml, and silwet-L77 was added to a final concentration of 0.02% before
518 spraying onto 3-week-old Arabidopsis seedlings. Bacterial numbers were determined
519 3 days post-inoculation as previously described (Macho *et al*., 2012; Wang *et al*.,
520 2019).

521

522 ***Ralstonia solanacearum* virulence assays**

523 For standard *R. solanacearum* virulence assays, 4-week-old *A. thaliana* plants, grown
524 in Jiffy pots, were inoculated with *R. solanacearum* without wounding by soil
525 drenching. For experiments using inducible transgenic lines, all the plants were
526 treated with 100 µM EST for 2 days before inoculation. Plants showed no difference in
527 root or shoot size at the time of inoculation. An overnight-grown bacterial suspension
528 was diluted to obtain an inoculum of $5x10^7$ cfu/ml. Once the Jiffy pots were completely
529 drenched, the plants were removed from the bacterial solution and placed back on a
530 bed of potting mixture soil. The genotypes to be tested were placed in a random order
531 in order to allow an unbiased analysis of the wilting. Daily scoring of the visible wilting
532 on a scale ranging from 0 to 4 (or 0 to 100% leaves wilting) led to an analysis using
533 the Kaplan-Meier survival analysis, log-rank test and hazard ratio calculation as
534 previously described (Morel et al., 2018b).

535 To determine *R. solanacearum* growth in Arabidopsis leaves, a 10^7 cfu/ml inoculum
536 was infiltrated into leaves of 4-week-old Arabidopsis plants 2 days after EST
537 treatment, and samples were taken 2 days after inoculation. To determine *R.*
538 *solanacearum* growth in *N. benthamiana* leaves, a 10^5 cfu/ml inoculum of *R.*

539 *solanacearum* Y45 was infiltrated into *N. benthamiana* leaves expressing RipE1-GFP
540 or a GFP control. RipE1-GFP was expressed using Agrobacterium, and *R.*
541 *solanacearum* Y45 was infiltrated in leaf tissues 24 hours after Agrobacterium
542 infiltration, before the development of cell death. *R. solanacearum* Y45 is a strain
543 originally isolated from tobacco (Li *et al*., 2011), which is pathogenic in *N.*
544 *benthamiana* (unpublished data). To determine bacterial numbers, leaf discs (3 leaf
545 discs from Arabidopsis plants and 4 leaf discs from *N. benthamiana* plants) were
546 taken and weighed. The plant tissue was ground and homogenized in distilled water
547 before plating serial dilutions to determine cfu per gram of fresh weight.
548

549 **Acknowledgements**

550 We thank Nemo Peeters and Anne-Claire Cazale for sharing unpublished biological
551 materials, Longjiang Fan, Yong Liu, Chanhong Kim, Alex Schultink, and Brian
552 Staskawicz for sharing biological materials, Rosa Lozano-Duran for critical reading of
553 this manuscript, and Xinyu Jian for technical and administrative assistance during this
554 work. We thank the PSC Cell Biology, Proteomics, and Metabolomics core facilities
555 for assistance with confocal microscopy and mass spectrometry analysis, respectively.
556 This work was supported by the Strategic Priority Research Program of the Chinese
557 Academy of Sciences (grant XDB27040204), the National Natural Science
558 Foundation of China (NSFC; grant 31571973), the Chinese 1000 Talents Program,
559 and the Shanghai Center for Plant Stress Biology (Chinese Academy of Sciences).
560 The authors have no conflict of interest to declare.

561

562

563 **References**

564 Azevedo, C., Sadanandom, A., Kitagawa, K., Freialdenhoven, A., Shirasu, K., and
565 Schulze-Lefert, P. (2002). The RAR1 interactor SGT1, an essential
566 component of *R* gene-triggered disease resistance. Science 295:2073-2076.
567 Bell E, Creelman RA, Mullet JE. (1995). A chloroplast lipoxygenase is required for
568 wound‐induced jasmonic acid accumulation in Arabidopsis. Proceedings of
569 the National Academy of Sciences, USA 92: 8675–8679.
570 Burger, M., and Chory, J. (2019). Stressed out about hormones: how plants
571 orchestrate immunity. Cell Host Microbe 26:163-172.
572 Catherine, D., Yves, M., Nicolas, D., Marine, C., Patrick, D., Philippe, R., Yves, M.,
573 Alain, J., and Deborah, G. (2012). Deciphering the route of *Ralstonia*
574 *solanacearum* colonization in *Arabidopsis thaliana* roots during a compatible
575 interaction: focus at the plant cell wall. Planta 236:1419-1431.
576 Chiang, Y.-H., and Coaker, G. (2015). Effector Triggered Immunity: NLR immune
577 perception and downstream defense responses. The Arabidopsis Book 2015.
578 Clarke, C.R., Studholme, D.J., Byron, H., Brendan, R., Alexandra, W., Rongman, C.,
579 Tadeusz, W., Marie-Christine, D., Emmanuel, W., and Castillo, J.A. (2015).
580 Genome-enabled phylogeographic investigation of the quarantine pathogen
581 *Ralstonia solanacearum* Race 3 Biovar 2 and screening for sources of
582 resistance against its core effectors. Phytopathology 105:597-607.
583 Cui, H., Tsuda, K., Parker, J.E. (2015). Effector-triggered immunity: from pathogen
584 perception to robust defense. In: Annual Review Plant Biology. 487-511.
585 Delaney, T.P., Uknes, S., Vernooij, B., Friedrich, L., Weymann, K., Negrotto, D.,
586 Gaffney, T., Gut-Rella, M., Kessmann, H., and Ward, E. (1994). A central role
587 of salicylic acid in plant disease resistance. Science 266:1247-1250.
588 Forcat, S., Bennett, M., Mansfield, J., and Grant, M. (2008). A rapid and robust
589 method for simultaneously measuring changes in the phytohormones ABA, JA
590 and SA in plants following biotic and abiotic stress. Plant methods 4:16.
591 Fujiwara, S., Kawazoe, T., Ohnishi, K., Kitagawa, T., Popa, C., Valls, M., Genin, S.,
592 Nakamura, K., Kuramitsu, Y., and Tanaka, N. (2016). RipAY, a plant pathogen
593 effector protein exhibits robust γ-glutamyl cyclotransferase activity when
594 stimulated by eukaryotic thioredoxins. Journal of Biological Chemistry
595 291:6813-6830.
596 Galán, J.E., Lara-Tejero, M., Marlovits, T.C., and Wagner, S. (2014). Bacterial type III
597 secretion systems: specialized nanomachines for protein delivery into target
598 cells. Annual Review of Microbiology 68:415-438.
599 Garcion, C., Lohmann, A., Lamodière, E., Catinot, J., Buchala, A., Doermann, P., and
600 Métraux, J.-P. (2008). Characterization and biological function of the
601 ISOCHORISMATE SYNTHASE2 gene of Arabidopsis. Plant Physiology
602 147:1279-1287.
603 Gassmann, W., ., Hinsch, M.E., and Staskawicz, B.J. (2010). The Arabidopsis RPS4
604 bacterial-resistance gene is a member of the TIR-NBS-LRR family of
605 disease-resistance genes. Plant Journal for Cell & Molecular Biology
606 20:265-277.

607 Gimenez-Ibanez, S., Boter, M., Fernández-Barbero, G., Chini, A., Rathjen, J.P., and
608 Solano, R. (2014). The bacterial effector HopX1 targets JAZ transcriptional
609 repressors to activate jasmonate signaling and promote infection in
610 Arabidopsis. PLoS Biology 12:e1001792-e1001792.
611 Gimenez-Ibanez, S., Chini, A., & Solano, R. (2016). How microbes twist jasmonate
612 signaling around their little fingers. Plants *(Basel, Switzerland)*, *5*: 9.
613 Jayaraman, J., Segonzac, C., Cho, H., Jung, G., and Sohn, K.H. (2016).
614 Effector-assisted breeding for bacterial wilt resistance in horticultural crops.
615 Horticulture Environment & Biotechnology 57:415-423.
616 Jiang, G., Wei, Z., Xu, J., Chen, H., Zhang, Y., She, X., Macho, A.P., Ding, W., and
617 Liao, B. (2017). Bacterial wilt in China: history, current status, and future
618 perspectives. Frontiers in Plant Science 8:1549.
619 Jones, J.D.G., and Dangl, J.L. (2006). The plant immune system. Nature
620 444:323-329.
621 Kadota, Y., Shirasu, K., and Guerois, R. (2010). NLR sensors meet at the SGT1–
622 HSP90 crossroad. Trends in biochemical sciences 35:199-207.
623 Lavie, M., Shillington, E., Eguiluz, C., Grimsley, N., and Boucher, C. (2002). PopP1, a
624 new member of the YopJ/AvrRxv family of type III effector proteins, acts as a
625 host-specificity factor and modulates aggressiveness of *Ralstonia*
626 *solanacearum*. Molecular Plant Microbe Interactions :15:1058-1068.
627 Leroux, C., Huet, G., Jauneau, A., Camborde, L., Trémousaygue, D., Kraut, A., Zhou,
628 B., Levaillant, M., Adachi, H., and Yoshioka, H. (2015). A receptor pair with an
629 integrated decoy converts pathogen disabling of transcription factors to
630 immunity. Cell 161:1074-1088.
631 Li Z, Wu S, Bai X, Liu Y, Lu J, Liu Y, Xiao B, Lu X, Fan L. (2011) Genome sequence of
632 the tobacco bacterial wilt pathogen Ralstonia solanacearum. Journal of
633 Bacteriology 193: 6088-6089.
634 Li, X. (2011). Infiltration of *Nicotiana benthamiana* protocol for transient expression via
635 Agrobacterium. Bio-protocol Bio101:e95.
636 Livak, K.J., and Schmittgen, T.D. (2001). Analysis of relative gene expression data
637 using real-time quantitative PCR and the 2(-Delta Delta C(T)) Method.
638 Methods 25:402-408.
639 Lv, R., Li, Z., Li, M., Dogra, V., Lv, S., Liu, R., Lee, K.P., and Kim, C. (2019)
640 Uncoupled expression of nuclear and plastid photosynthesis-associated
641 genes contributes to cell death in a lesion mimic mutant. Plant Cell 31: 210–
642 230.
643 Macho, A.P., Boutrot, F., Rathjen, J.P., and Zipfel, C. (2012). ASPARTATE OXIDASE
644 plays an important role in Arabidopsis stomatal immunity. Plant Physiology
645 159: 1845-1856.
646 Macho, A.P. (2016). Subversion of plant cellular functions by bacterial type-III
647 effectors: beyond suppression of immunity. New Phytologist 210:51-57.
648 Macho, A.P., and Zipfel, C. (2015). Targeting of plant pattern recognition
649 receptor-triggered immunity by bacterial type-III secretion system effectors.
650 Current Opinion in Microbiology 23:14-22.

651 Makarova, K.S., Aravind, L., and Koonin, E.V. (1999). A superfamily of archaeal,
652 bacterial, and eukaryotic proteins homologous to animal transglutaminases.
653 Protein Science 8:1714-1719.
654 Manifield, John, GENIN, Stephane, MAGORI, Shimpei, CITOVSKY, Vitaly, and
655 SRIARIYANUM. (2012). Top 10 plant pathogenic bacteria in molecular plant
656 pathology. Molecular Plant Pathology 13:614-629.
657 Mansfield, J., Jenner, C., Hockenhull, R., Bennett, M.A., and Stewart, R. (1994).
658 Characterization of avrPphE, a gene for cultivar-specific avirulence from
659 *Pseudomonas syringae* pv. *phaseolicola* which is physically linked to hrpY, a
660 new hrp gene identified in the halo-blight bacterium. Molecular Plant Microbe
661 Interaction 7:726-739.
662 Morel A, G.J., Lonjon F, Sujeeun L, Barberis P, Genin S, Vailleau F, Daunay MC,
663 Dintinger J, Poussier S, Peeters N, Wicker E. (2018a). The eggplant AG91-25
664 recognizes the Type III-secreted effector RipAX2 to trigger resistance to
665 bacterial wilt (*Ralstonia solanacearum* species complex). Molecular Plant
666 Pathology 19:2459-2472.
667 Morel, A., Peeters, N., Vailleau, F., Barberis, P., Jiang, G., Berthomé, R., and Guidot,
668 A. (2018b). Plant pathogenicity phenotyping of *Ralstonia solanacearum*
669 strains. in: Host-Pathogen Interactions: Methods and Protocols--Medina, C.,
670 and López-Baena, F.J., eds. New York, NY: Springer New York. 223-239.
671 Mukaihara, T., Hatanaka, T., Nakano, M., and Oda, K. (2016). *Ralstonia*
672 *solanacearum* Type III effector RipAY is a glutathione-degrading enzyme that
673 is activated by plant cytosolic thioredoxins and suppresses plant immunity.
674 Mbio 7:e00359.
675 Mukaihara, T., Tamura, N., and Iwabuchi, M. (2010). Genome-wide identification of a
676 large repertoire of *Ralstonia solanacearum* type III effector proteins by a new
677 functional screen. Molecular Plant Microbe Interaction 23:251-262.
678 Nahar, K., Matsumoto, I., Taguchi, F., Inagaki, Y., Yamamoto, M., Toyoda, K.,
679 Shiraishi, T., Ichinose, Y., and Mukaihara, T. (2014). *Ralstonia solanacearum*
680 type III secretion system effector Rip36 induces a hypersensitive response in
681 the nonhost wild eggplant *Solanum torvum*. Molecular Plant Pathology
682 15:297-303.
683 Nakagawa, T., Suzuki, T., Murata, S., Nakamura, S., Hino, T., Maeo, K., Tabata, R.,
684 Kawai, T., Tanaka, K., and Niwa, Y. (2007). Improved Gateway binary vectors:
685 high-performance vectors for creation of fusion constructs in transgenic
686 analysis of plants. Journal of the Agricultural Chemical Society of Japan
687 71:2095-2100.
688 Nakano M, Mukaihara T. (2019). The type III effector RipB from *Ralstonia*
689 *solanacearum* RS1000 acts as a major avirulence factor in *Nicotiana*
690 *benthamiana* and other Nicotiana species. Molecular Plant Pathology
691 20:1237-1251.
692 Nakano, M., and Mukaihara, T. (2018). *Ralstonia solanacearum* Type III effector
693 RipAL targets chloroplasts and induces jasmonic acid production to suppress

694 salicylic acid-mediated defense responses in plants. Plant and Cell Physiology
695 59:2576-2589.
696 Nimchuk, Z.L., Fisher, E.J., Desveaux, D., Chang, J.H., and Dangl, J.L. (2007). The
697 HopX (AvrPphE) family of *Pseudomonas syringae* type III effectors require a
698 catalytic triad and a novel N-terminal domain for function. Molecular Plant
699 Microbe Interactions 20:346-357.
700 Peeters, N., Carrère, S., Anisimova, M., Plener, L., Cazalé, A.C., and Genin, S.
701 (2013a). Repertoire, unified nomenclature and evolution of the Type III effector
702 gene set in the *Ralstonia solanacearum* species complex. BMC Genomics
703 14:859-859.
704 Peeters, N., Guidot, A., Vailleau, F., and Valls, M. (2013b). *Ralstonia solanacearum*, a
705 widespread bacterial plant pathogen in the post-genomic era. Molecular Plant
706 Pathology 14:651–662.
707 Poueymiro, M., Cunnac, S., Barberis, P., Deslandes, L., Peeters, N., Cazale-Noel,
708 A.C., Boucher, C., and Genin, S. (2009). Two type III secretion system
709 effectors from *Ralstonia solanacearum* GMI1000 determine host-range
710 specificity on tobacco. Molecular Plant Microbe Interaction 22:538-550.
711 Rosas-Díaz, T., Cana-Quijada, P., Amorim-Silva, V., Botella, M.A., Lozano-Durán, R.,
712 and Bejarano, E.R. (2017). *Arabidopsis NahG* plants as a suitable and
713 efficient system for transient expression using *Agrobacterium tumefaciens*.
714 Molecular Plant 10:353-356.
715 Rufián, J.S, Lucía, A, Rueda-Blanco, J, Zumaquero, A, Guevara, C.M, Ortiz-Martín, I,
716 Ruiz-Aldea, G, Macho, A.P, Beuzón, C.R, and Ruiz-Albert J (2018)
717 Suppression of HopZ effector-triggered plant immunity in a natural
718 pathosystem. Frontiers in Plant Sciences 9:977-981.
719 Sang, Y., and Macho, A.P. (2017). Analysis of PAMP-triggered ROS burst in plant
720 immunity. Methods in Molecular Biology 1578:143-153.
721 Sang, Y., Wang, Y., Ni, H., Cazalã, A.C., She, Y.M., Peeters, N., and Macho, A.P.
722 (2016). The *Ralstonia solanacearum* type III effector RipAY targets plant redox
723 regulators to suppress immune responses. Molecular Plant Pathology
724 19:129-142.
725 Sarris, P., Duxbury, Z., Huh, S.U., Ma, Y., Segonzac, C., Sklenar, J., Derbyshire, P.,
726 Cevik, V., Rallapalli, G., and Saucet, S. (2015). A plant immune receptor
727 detects pathogen effectors that target WRKY transcription factors. Cell
728 161:1089-1100.
729 Schlücking, K., Kai, H.E., Köster, P., Drerup, M.M., Eckert, C., Steinhorst, L., Waadt,
730 R., Batistič, O., and Kudla, J. (2013). A new β-estradiol-inducible vector set
731 that facilitates easy construction and efficient expression of transgenes
732 reveals CBL3-dependent cytoplasm to tonoplast translocation of CIPK5.
733 Molecular Plant 6:1814-1829.
734 Schultink, A., Qi, T., Lee, A., Steinbrenner, A.D., and Staskawicz, B. (2017). Roq1
735 mediates recognition of the Xanthomonas and Pseudomonas effector proteins
736 XopQ and HopQ1. Plant Journal 92:787-795

737 Segonzac, C., Feike, D., Gimenez Ibanez, S., Dagmar R, H., Zipfel, C., and John P,
738 R. (2011). Hierarchy and roles of pathogen-associated molecular
739 pattern-induced responses in Nicotiana benthamiana. Plant Physiology
740 156:687-699.
741 Senthil-Kumar, M., and Mysore, K.S. (2014). Tobacco rattle virus–based
742 virus-induced gene silencing in Nicotiana benthamiana. Nature Protocols
743 9:1549-1562.
744 Shine, M.B., Yang, J.W., El‐Habbak, M., Nagyabhyru, P., Fu, D.Q., Navarre, D.,
745 Ghabrial, S., Kachroo, P., and Kachroo, A. (2016). Cooperative functioning
746 between phenylalanine ammonia lyase and isochorismate synthase activities
747 contributes to salicylic acid biosynthesis in soybean. New Phytologist
748 212:627-636.
749 Solé, M., Popa, C., Mith, O., Sohn, K.H., Jones, J., Deslandes, L., and Valls, M.
750 (2012). The awr gene family encodes a novel class of *Ralstonia solanacearum*
751 type III effectors displaying vrulence and avirulence activities. Molecular Plant
752 Microbe Interactions 25:941-953.
753 Stevens, C., Bennett, M.A., Athanassopoulos, E., Tsiamis, G., Taylor, J.D., and
754 Mansfield, J.W. (1998). Sequence variations in alleles of the avirulence gene
755 avrPphE.R2 from *Pseudomonas syringae* pv. *phaseolicola* lead to loss of
756 recognition of the AvrPphE protein within bean cells and a gain in
757 cultivar-specific virulence. Molecular Microbiology 29:165-177.
758 Tasset, C., Bernoux, M., Jauneau, A., Pouzet, C., Brière, C., Kieffer-Jacquinod, S.,
759 Rivas, S., Marco, Y., and Deslandes, L. (2010). Autoacetylation of the
760 *Ralstonia solanacearum* effector PopP2 targets a lysine residue essential for
761 RRS1-R-mediated immunity in Arabidopsis. PLOS Pathogens 6:e1001202.
762 Turner, M., Jauneau, A., Genin, S., Tavella, M.J., Vailleau, F., Gentzbittel, L., and
763 Jardinaud, M.F. (2009). Dissection of bacterial wilt on *Medicago truncatula*
764 revealed two type III secretion system effectors acting on root infection
765 process and disease development. Plant Physiology 150:1713-1722.
766 Vlot, A.C., Dempsey, D.M.A., and Klessig, D.F. (2009). Salicylic acid, a multifaceted
767 hormone to combat disease. Annual Review of Phytopathology 47:177-206.
768 Wang, Y., Li, Y., Rosas-Diaz, T., Caceres-Moreno, C., Lozano-Durán, R., and Macho,
769 A.P. (2019). The IMMUNE-ASSOCIATED NUCLEOTIDE-BINDING 9 protein
770 is a regulator of basal immunity in *Arabidopsis thaliana*. Molecular Plant
771 Microbe Interactions 32:65-75.
772 Ward, E.R., Uknes, S.J., Williams, S.C., Dincher, S.S., Wiederhold, D.L., Alexander,
773 D.C., Ahlgoy, P., Métraux, J.P., and Ryals, J.A. (1991). Coordinate gene
774 activity in response to agents that induce systemic acquired resistance. Plant
775 Cell 3:1085-1094.
776 Wei, Y., Caceres-Moreno, C., Jimenez-Gongora, T., Wang, K., Sang, Y.,
777 Lozano-Duran, R., and Macho, A.P. (2017). The *Ralstonia solanacearum*
778 csp22 peptide, but not flagellin-derived peptides, is perceived by plants from
779 the Solanaceae family. Plant Biotechnology Journal 16:1349-1362

780 Wiermer, Marcel, FEYS, Bart, J., PARKER, and Jane, E. (2005). Plant immunity : the
781 EDS1 regulatory node. Current Opinion in Plant Biology 8:383-389.
782 Wildermuth, M.C., Dewdney, J., ., Wu, G., ., and Ausubel, F.M. (2001). Isochorismate
783 synthase is required to synthesize salicylic acid for plant defence. Nature
784 414:562-565.
785 Williams, S.J., Kee Hoon, S., Li, W., Maud, B., Sarris, P.F., Cecile, S., Thomas, V.,
786 Yan, M., Saucet, S.B., and Ericsson, D.J. (2014). Structural basis for
787 assembly and function of a heterodimeric plant immune receptor. Science
788 344:299-303.
789 Wu, C.-H., Abd-El-Haliem, A., Bozkurt, T.O., Belhaj, K., Terauchi, R., Vossen, J.H.,
790 and Kamoun, S. (2017). NLR network mediates immunity to diverse plant
791 pathogens. Proceedings of the National Academy of Sciences USA
792 114:8113-8118.
793 Wu, C.H., Belhaj, K., Bozkurt, T.O., Birk, M.S., and Kamoun, S. (2016). Helper NLR
794 proteins NRC2a/b and NRC3 but not NRC1 are required for Pto-mediated cell
795 death and resistance in *Nicotiana benthamiana*. New Phytologist
796 209:1344-1352.
797 Yu, G., Xian, L., Sang, Y., and Macho, A.P. (2019a). Cautionary notes on the use of
798 Agrobacterium-mediated transient gene expression upon SGT1 silencing in
799 *Nicotiana benthamiana*. New Phytologist 222:14-17.
800 Yu, G., Xian, L., Xue, H., Yu, W., Rufian, J., Sang, Y., Morcillo, R., Wang, Y., and
801 Macho, A.P. (2019b). A bacterial effector protein prevents MAPK-mediated
802 phosphorylation of SGT1 to suppress plant immunity. bioRxiv:641241.
803 Zhang, X., Henriques, R., Lin, S.-S., Niu, Q.-W., and Chua, N.-H. (2006).
804 Agrobacterium-mediated transformation of *Arabidopsis thaliana* using the
805 floral dip method. Nature Protocols 1:641-646.
806

807 **Figure legends**

808 **Figure 1. RipE1 triggers cell death in *Nicotiana benthamiana*.**

809 (a) RipE1-GFP or GFP (as control) were expressed in the same leaf of *N.*
810 *benthamiana* using Agrobacterium with an OD_{600} of 0.5. Photos were taken 2 days
811 post-inoculation with a CCD camera (upper panel) or an UV camera (lower panel). UV
812 signal corresponds to the development of cell death (not GFP fluorescence). UV
813 images were taken from the abaxial side and flipped horizontally for representation. (b)
814 Ion leakage measured in leaf discs taken from *N. benthamiana* tissues expressing
815 RipE1-GFP or GFP (as control), representative of cell death, at the indicated time
816 points. Values indicate mean ± SE (n=3 biological replicates). (c) Simplified diagram
817 of RipE1, including the residues comprising the Domain A and the predicted catalytic
818 triad. (d) Western blot showing the accumulation of RipE1 mutant variants. ΔAD
819 corresponds to a deletion mutant of the Domain A (residues 121-128). Molecular
820 weight (kDa) marker bands are indicated for reference. (e) Cell death triggered by
821 RipE1 mutant variants (conditions as in (a)). (f) Ion leakage measured in leaf discs
822 taken from *N. benthamiana* tissues expressing RipE1 mutant variants (conditions as
823 in (b). Each experiment was repeated at least 3 times with similar results.

824

825 **Figure 2. RipE1 activates SA-dependent immune responses in *N. benthamiana*.**

826 (a) Quantitative RT-PCR to determine the expression of *RipE1* and *NbPR1* in *N.*
827 *benthamiana* tissues expressing GFP, RipE1, or RipE1 C172A, using Agrobacterium
828 with an OD_{600} of 0.1. Samples were taken at the indicated times after Agrobacterium
829 infiltration. In each case, the RipE1 variants and their respective GFP control were
830 expressed in the same leaf, and values are represented side-by-side. Expression
831 values are relative to the expression of the housekeeping gene *NbEF1a*. Values
832 indicate mean ± SE (n=3 biological replicates). (b) RipE1-GFP or GFP (as control)
833 were expressed in the same leaf of *N. benthamiana* using Agrobacterium with an
834 OD_{600} of 0.5. Twenty-four hours after Agrobacterium infiltration, before the
835 appearance of cell death, a 10^5 cfu/ml inoculum of *R. solanacearum* Y45 was
836 infiltrated into the same tissues. Samples were taken one day post-inoculation to

837 determine Y45 colony-forming units (cfu) per gram of tissue. Values indicate mean ±
838 SE (n=6 biological replicates). (c-e) RipE1-Nluc was co-expressed with GFP (as
839 control) or with NahG-GFP in the same leaf. Protein accumulation is shown in the
840 figure S4. (c) Photos were taken 2.5 days post-inoculation with a CCD camera (upper
841 panel) or an UV camera (lower panel). UV signal corresponds to the development of
842 cell death (not GFP fluorescence). UV images were taken from the abaxial side and
843 flipped horizontally for representation. (d) Ion leakage measured in leaf discs taken
844 from *N. benthamiana* tissues expressing RipE1 together with GFP or NahG-GFP,
845 representative of cell death, at the indicated time points. Values indicate mean ± SE
846 (n=3 biological replicates). (e) Quantitative RT-PCR to determine the expression of
847 *NbPR1* in *N. benthamiana* tissues 48 hours after Agrobacterium infiltration.
848 Expression values are relative to the expression of the housekeeping gene *NbEF1a*.
849 Values indicate mean ± SE (n=3 biological replicates). Asterisks indicate significant
850 differences compared to the mock control according to a Student's t test (* $p < 0.05$;
851 *** $p < 0.001$). Each experiment was repeated at least 3 times with similar results.
852
853 **Figure 3. RipE1 perception enhances the expression of *PAL* genes and SA**
854 **biosynthesis in *N. benthamiana*.**
855 (a) Measurement of SA accumulation in *N. benthamiana* tissues expressing GFP,
856 RipE1, or RipE1 C172A, using Agrobacterium with an OD_{600} of 0.5. Samples were
857 taken 42 hours after Agrobacterium infiltration. Three independent biological repeats
858 were performed, and the different colors indicate values from different replicates.
859 Values are represented as % of the GFP control in each replicate. (b-f) Quantitative
860 RT-PCR to determine the expression of *NbICS1* (b), *NbPAL05* (c), *NbPAL08* (d),
861 *NbPAL10* (e), and *NbLOX2* (f) in *N. benthamiana* tissues expressing GFP, RipE1, or
862 RipE1 C172A, using Agrobacterium with an OD_{600} of 0.5. Samples were taken at the
863 indicated times after Agrobacterium infiltration. In each case, the RipE1 variants and
864 their respective GFP control were expressed in the same leaf, and values are
865 represented side-by-side. *NbPAL05:* Niben101Scf05617g00005.1; *NbPAL08*:
866 Niben101Scf03712g01008.1; *NbPAL10:* Niben101Scf12881g00010.1. Expression

867 values are relative to the expression of the housekeeping gene *NbEF1a*. Values
868 indicate mean ± SE (n=3 biological replicates). Asterisks indicate significant
869 differences compared to the mock control according to a Student's t test (* $p < 0.05$; **
870 $p < 0.01$; *** $p < 0.001$). Each experiment was repeated at least 3 times with similar
871 results.
872
873 **Figure 4. RipE1-triggered responses require SGT1, but not EDS1.**
874 (a-d) RipE1-GFP or GFP (as control) were expressed in the same leaf of *N.*
875 *benthamiana* undergoing VIGS of *NbSGT1* or VIGS with an empty vector (EV)
876 construct (as control), using Agrobacterium with an OD_{600} of 0.5. (a) Western blot
877 showing the accumulation of GFP, RipE1-GFP, and endogenous *NbSGT1*. Molecular
878 weight (kDa) marker bands are indicated for reference. (b) Photos were taken 2 days
879 post-inoculation with a CCD camera (upper panel) or an UV camera (lower panel). UV
880 signal corresponds to the development of cell death (not GFP fluorescence). UV
881 images were taken from the abaxial side and flipped horizontally for representation. (c)
882 Ion leakage measured in leaf discs taken from *N. benthamiana* tissues expressing
883 RipE1-GFP or GFP (as control), representative of cell death, 48 hours after
884 Agrobacterium infiltration. Values indicate mean ± SE (n=3 biological replicates). (d)
885 Quantitative RT-PCR to determine the expression of *NbPR1* in *N. benthamiana*
886 tissues 48 hours after Agrobacterium infiltration. Expression values are relative to the
887 expression of the housekeeping gene *NbEF1a*. Values indicate mean ± SE (n=3
888 biological replicates). (e) RipE1-GFP or GFP (as control) were expressed in the same
889 leaf of *N. benthamiana* wild type or a stable *eds1* knockout mutant, using
890 Agrobacterium with an OD_{600} of 0.5. Photos were taken 2 days post-inoculation with a
891 CCD camera (upper panel) or an UV camera (lower panel). UV signal corresponds to
892 the development of cell death (not GFP fluorescence). UV images were taken from
893 the abaxial side and flipped horizontally for representation. Asterisks indicate
894 significant differences compared to the mock control according to a Student's t test
895 (*** $p < 0.001$). Each experiment was repeated at least 3 times with similar results.
896

897 **Figure 5. RipE1 triggers immunity in Arabidopsis.**

898 (a) Arabidopsis Col-0 wild type or independent stable transgenic lines expressing
899 RipE1 or RipE1 C172A from an estradiol (EST)-inducible promoter were grown for 3
900 weeks and then treated sprayed with 100 μM EST daily. Photographs were taken 2
901 weeks after beginning the EST treatment. (b) Arabidopsis 4 day-old seedlings were
902 treated with 25 μM EST and samples were taken 1, 2, 3, or 4 days after EST
903 treatment. Quantitative RT-PCR to determine the expression of *RipE1, AtPR1,*
904 *AtPAL1, AtICS1, AtVSP2,* and *AtPDF1.2*. Expression values are relative to the
905 expression of the housekeeping gene *AtACT2*. Values indicate mean ± SE (n=3
906 biological replicates). (c) Arabidopsis Col-0 wild type or EST-RipE1 transgenic plants
907 were grown for 4 weeks and then treated with 100 μM EST for 2 days before
908 inoculation with *R. solanacearum* GMI1000 by soil-drenching. Plants showed no
909 difference in root or shoot size at the time of inoculation. The results are represented
910 as disease progression, showing the average wilting symptoms in a scale from 0 to 4
911 (mean ± SEM). n=20 plants per genotype. Asterisks indicate significant differences
912 compared to the mock control according to a Student's t test (* $p < 0.05$; ** $p < 0.01$;
913 *** $p < 0.001$). Each experiment was repeated at least 3 times with similar results.

914

915 **Figure 6. RipE1-triggered immune responses are suppressed by RipAY.**

916 (a) RipE1-GFP or GFP (as control) were expressed in the same leaf of *N.*
917 *benthamiana* using Agrobacterium with an OD_{600} of 0.5, and samples were taken at
918 the indicated time points to measure the accumulation of glutathione (GSH). (b-d)
919 RipE1-Nluc was co-expressed with GFP (as control), with RipAY-GFP, or with
920 RipAY-E216Q-GFP, respectively, in the same leaf. Protein accumulation is shown in
921 the figure S8. (b) Photos were taken 2.5 days post-inoculation with a CCD camera
922 (upper panel) or an UV camera (lower panel). UV signal corresponds to the
923 development of cell death (not GFP fluorescence). UV images were taken from the
924 abaxial side and flipped horizontally for representation. (c) Ion leakage measured in
925 leaf discs taken from *N. benthamiana* tissues expressing RipE1 together with GFP or
926 RipAY-GFP, representative of cell death, at the indicated time points. Values indicate

927 mean ± SE (n=3 biological replicates). (d) Quantitative RT-PCR to determine the
928 expression of *NbPR1* in *N. benthamiana* tissues 48 hours after Agrobacterium
929 infiltration. Expression values are relative to the expression of the housekeeping gene
930 *NbEF1a*. Values indicate mean ± SE (n=3 biological replicates). Asterisks indicate
931 significant differences compared to the mock control according to a Student's t test (*
932 $p < 0.05$; *** $p < 0.001$). Each experiment was repeated at least 3 times with similar
933 results.
934
935 **Figure S1. Phylogenetic analysis of RipE1**
936 Alignment of the amino acid sequence of RipE1 from *R. solanacearum* GMI1000
937 (Rs_RipE1), XopE1 from *Xanthomonas campestris* pv. *vesicatoria* (Xs_XopE1), and
938 HopX1 from *Pseudomonas syringae* pv tabaci 11528 (Ps_HopX1). Residues forming
939 the predicted catalytic triad are indicated in red, and the conserved domain A is
940 indicated in blue. The black shaded amino acids are identical among the three
941 effectors.
942
943 **Figure S2. RipE1 induces cell death in *N. benthamiana.***
944 RipE1-GFP, RipE1-C172A-GFP, RipAA-GFP, and GFP (as control) were expressed
945 in the same leaf of *N. benthamiana* using Agrobacterium with an OD_{600} of 0.5. (a)
946 Trypan blue staining was performed 4 days post-inoculation, and additional photos of
947 an independent unstained leaf is shown for reference. (b) Ion leakage measured in
948 leaf discs taken from *N. benthamiana* tissues expressing the indicated constructs, at
949 the indicated time points. Values indicate mean ± SE (n=3 biological replicates).
950 These experiments were repeated 3 times with similar results.
951
952 **Figure S3. RipE1 expression inhibits PTI responses in *N. benthamiana*, which**
953 **correlates with the induction of cell death.**
954 Agrobacterium was used to induce the transient expression of RipE1-GFP in half of
955 the leaf and GFP in the other half. (a) Oxidative burst triggered by 50 nM flg22 in *N.*
956 *benthamiana* tissues at the indicated time points, measured in a luminol-based assay

957 as relative luminescence units (RLU). Values are average ± SE (n=24), and are
958 represented as % of the GFP control in each time point. Western blot with anti-GFP is
959 shown for reference of protein accumulation at each time point. (b) MAPK activation
960 was induced 40 hours after Agrobacterium infiltration with 100 nM flg22 and analysed
961 15 minutes after flg22 treatment using anti-phosphorylated MAPK antibody
962 (anti-pMAPK). Immunoblots were also analysed using anti-GFP antibody to verify
963 protein accumulation. Anti-actin was used to verify equal loading. Molecular weight
964 (kDa) marker bands are indicated for reference. (c) Oxidative burst was induced as in
965 (a) and measured 2 days post-Agrobacterium infiltration. Mutant variants are
966 described in the Figure 1. (d) Ion leakage was measured as in the Figure 1.
967 Measurement over time after RipE1 expression reflects that the induction of cell death
968 correlates in time with the suppression of PTI responses. The experiments were
969 repeated three times with similar results.
970
971 **Figure S4. Protein accumulation upon co-expression of RipE1 and NahG.**
972 Western blot showing protein accumulation in the experiments shown in the figure 2.
973 Molecular weight (kDa) marker bands are indicated for reference.
974
975 **Figure S5. RipE1 expression leads to an increase in JA contents.**
976 Measurement of JA accumulation in *N. benthamiana* tissues expressing GFP or
977 RipE1, using Agrobacterium with an OD_{600} of 0.5. Samples were taken 42 hours after
978 Agrobacterium infiltration. Three independent biological repeats were performed, and
979 the different colors indicate values from different replicates. Values are represented
980 as % of the GFP control in each replicate.
981
982 **Figure S6. RipE1-triggered cell death does not require NRC proteins.**
983 RipE1-GFP, RipE1-C172A-GFP or GFP (as control) were transiently expressed using
984 agrobacterium into wild type (WT) *N. benthamiana*, leaves silenced with EV (as
985 control) and those silenced with different NRC homologs (NRC2/3, NRC4 and
986 NRC2/3/4-Triple), using VIGS. For RipE1-GFP, RipE1-C172A-GFP and GFP an

987 OD_{600} of 0.5 was used. Rpiblb2 (OD_{600} 0.2)/AVRblb2 (OD_{600} 0.1) and Pto (OD_{600}
988 0.6)/AVRPto (OD_{600} 0.1), which are NRC4 and NRC2/3 dependent, respectively, were
989 included as controls. Photos were taken 5 days post inoculation under natural or UV
990 light. UV images were taken from the abaxial side and flipped horizontally for
991 representation.
992
993 **Figure S7. Leaves of RipE1-expressing Arabidopsis plants show enhanced**
994 **resistance against inoculation with *R. solanacearum*, but not *P. syringae pv***
995 ***tomato* (*Pto*) DC3000.**
996 (a) Growth of *R. solanacearum* GMI1000 (inoculated at 10^7 cfu/ml) infiltrated with a
997 needleless syringe into wild-type Col-0 and RipE1-expressing Arabidopsis plants.
998 Four-week-old plants were sprayed with 100 µM estradiol and then covered for 2 days
999 prior inoculation. Bacterial colony-forming units (cfu) were determined 2 days
1000 post-inoculation (dpi). Values indicate mean ± SE (n=6 biological replicates).
1001 Asterisks indicate significant differences compared to Col-0 WT plants according to a
1002 Student's t test (** $p < 0.01$). A specific p value is indicated for the RipE1#1 plant to
1003 indicate a reproducible (but not statistically significant) difference in bacterial growth
1004 compared to Col-0 WT plants. (b) Growth of surface (spray)-inoculated *Pto* DC3000
1005 (inoculated at 10^8 cfu/ml) in wild-type Col-0 and RipE1-expressing Arabidopsis
1006 seedlings. Three-week-old seedlings were sprayed with 100 µM estradiol and then
1007 covered for 2 days prior inoculation. Bacterial colony-forming units (cfu) were
1008 determined 3 days post-inoculation (dpi). Values indicate mean ± SE (n=8 biological
1009 replicates). (c) Growth of *Pto* DC3000 (inoculated at 10^5 cfu/ml) infiltrated with a
1010 needleless syringe into wild-type Col-0 and RipE1-expressing Arabidopsis plants.
1011 Four-week-old plants were sprayed with 100 µM estradiol and then covered for 2 days
1012 prior inoculation. Bacterial colony-forming units (cfu) were determined 3 days
1013 post-inoculation (dpi). Values indicate mean ± SE (n=4 biological replicates).
1014 Experiments were repeated more than three times with similar results.
1015
1016 **Figure S8. Protein accumulation upon co-expression of RipE1 and RipAY.**

1017 Western blot showing protein accumulation in the experiments shown in the figure 6.
1018 Molecular weight (kDa) marker bands are indicated for reference.
1019
1020 **Figure S9. RipAY suppresses the overexpression of SA-related genes triggered**
1021 **by RipE1**
1022 Quantitative RT-PCR to determine the expression of *NbPAL05, NbPAL08, NbPAL10,*
1023 and *NbLOX2* in *N. benthamiana* tissues 48 hours after Agrobacterium infiltration.
1024 *NbPAL05:* Niben101Scf05617g00005.1; *NbPAL08*: Niben101Scf03712g01008.1;
1025 *NbPAL10:* Niben101Scf12881g00010.1. Expression values are relative to the
1026 expression of the housekeeping gene *NbEF1a*. Values indicate mean ± SE (n=3
1027 biological replicates). Asterisks indicate significant differences compared to the mock
1028 control according to a Student's t test (* $p < 0.05$).
1029

1030 **Table S1**: Primers used in this study for RipE1 cloning and qRT-PCR.

Gene	Forward primers	Reverse primers
Primers for site-directed amino acid mutation		
RipE1-C172A	AGGGGCGGGGAACGCCGGCGAACACGCC	GGCGTGTTCGCCGGCGTTCCCCGCCCCT
RipE1 ΔAD	GATACTGACGCACATCGACGCCACCCA	TGGGTGGCGTCGATGTGCGTCAGTATC
Primers for qRT-PCR in *N. benthamiana*		
NbEF1a	CCCAAGAGGCCCTCAGACA	CACACGACCAACAGGGACAGT
NbPR-1	GGTCAACACGGCGAAAACC	GCCTTAGCAGCCGTCATGA
NbICS1	GTGTCGGCTCTGCTGTCTTCT	CTGCGTATAGCACGCCAATC
NbPAL05	AAGGGAGCTGAAATCGCCAT	TCCGCACTTTGGACATGGTT
NbPAL08	TATCACCCCATGCTTGCCTC	AGTGGCCTTGGAATTGGGTC
NbPAL10	GTCACTCCATGTTTGCCCCT	GACCTGTGAGTAAACCGGCA
NbLOX2	TCTTGGGTGGCTCCTCTGACT	TGTTGGAGGTCTGCCTGTTCT
Primers for qRT-PCR in *A. thaliana*		
AtACTIN2	TGCTGGACGTGACCTTACTG	TTCTCGATGGAAGAGCTGGT
AtPR1	TGATCCTCGTGGGAATTATGT	TGCATGATCACATCATTACTTCAT
AtICS1	GCGTCGTTCGGTTACAGG	ACAGCGAGGCTGAATCTCAT
AtPAL1	TATCCCGAACAGGATCAAGG	TCTCCGGTCAAAAGCTCTGT
AtPDF1.2	ACTATGTCTTCCCAGCACAC	AACAACAACGGGAAAATAAA
AtVSP2	GTTTGGATCTTTGACCTAGACGA	CTCTAACCACGACCAGTACGC
Primers for cloning RipE1 to sXVE:GFPc:Bar estradiol inducible vector		
RipE1	TCAGGATCCATGCCGCCCGTCCTGCCGT	ACTCTCGAGGCTTTCCGTGGCGGGCGGCT

1031

Figure 1

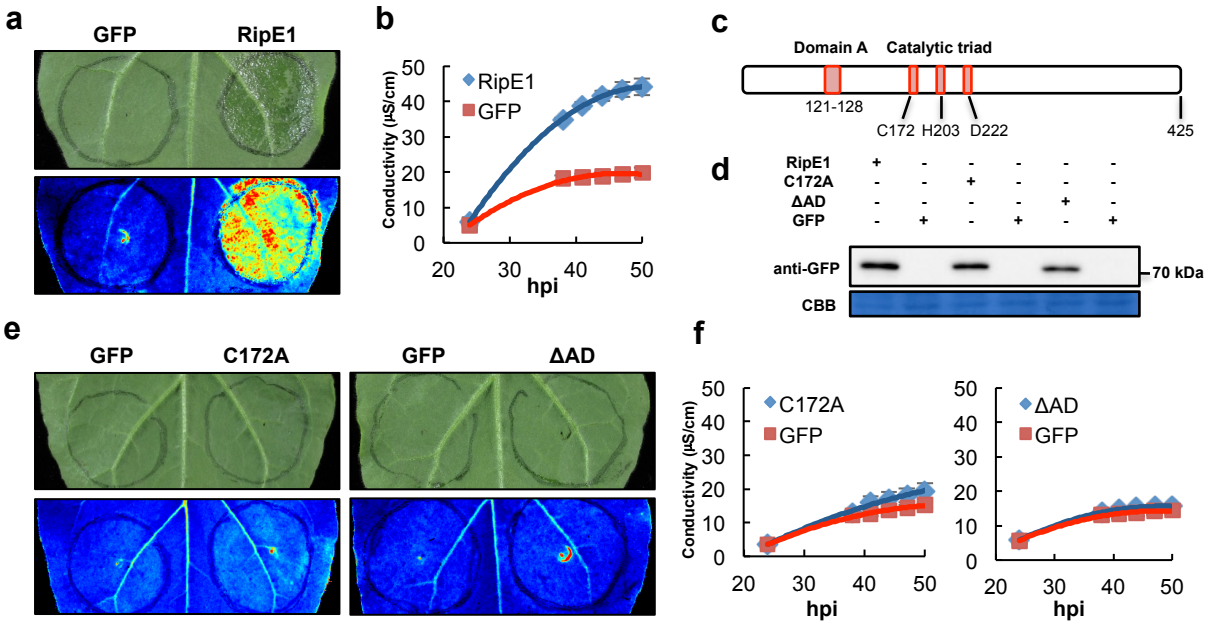

Figure 1. RipE1 triggers cell death in *Nicotiana benthamiana*.
(a) RipE1-GFP or GFP (as control) were expressed in the same leaf of *N. benthamiana* using Agrobacterium with an OD_{600} of 0.5. Photos were taken 2 days post-inoculation with a CCD camera (upper panel) or an UV camera (lower panel). UV signal corresponds to the development of cell death (not GFP fluorescence). UV images were taken from the abaxial side and flipped horizontally for representation. (b) Ion leakage measured in leaf discs taken from *N. benthamiana* tissues expressing RipE1-GFP or GFP (as control), representative of cell death, at the indicated time points. Values indicate mean ± SE (n=3 biological replicates). (c) Simplified diagram of RipE1, including the residues comprising the Domain A and the predicted catalytic triad. (d) Western blot showing the accumulation of RipE1 mutant variants. ΔAD corresponds to a deletion mutant of the Domain A (residues 121-128). Molecular weight (kDa) marker bands are indicated for reference. (e) Cell death triggered by RipE1 mutant variants (conditions as in (a)). (f) Ion leakage measured in leaf discs taken from *N. benthamiana* tissues expressing RipE1 mutant variants (conditions as in (b)). Each experiment was repeated at least 3 times with similar results.

Figure 2

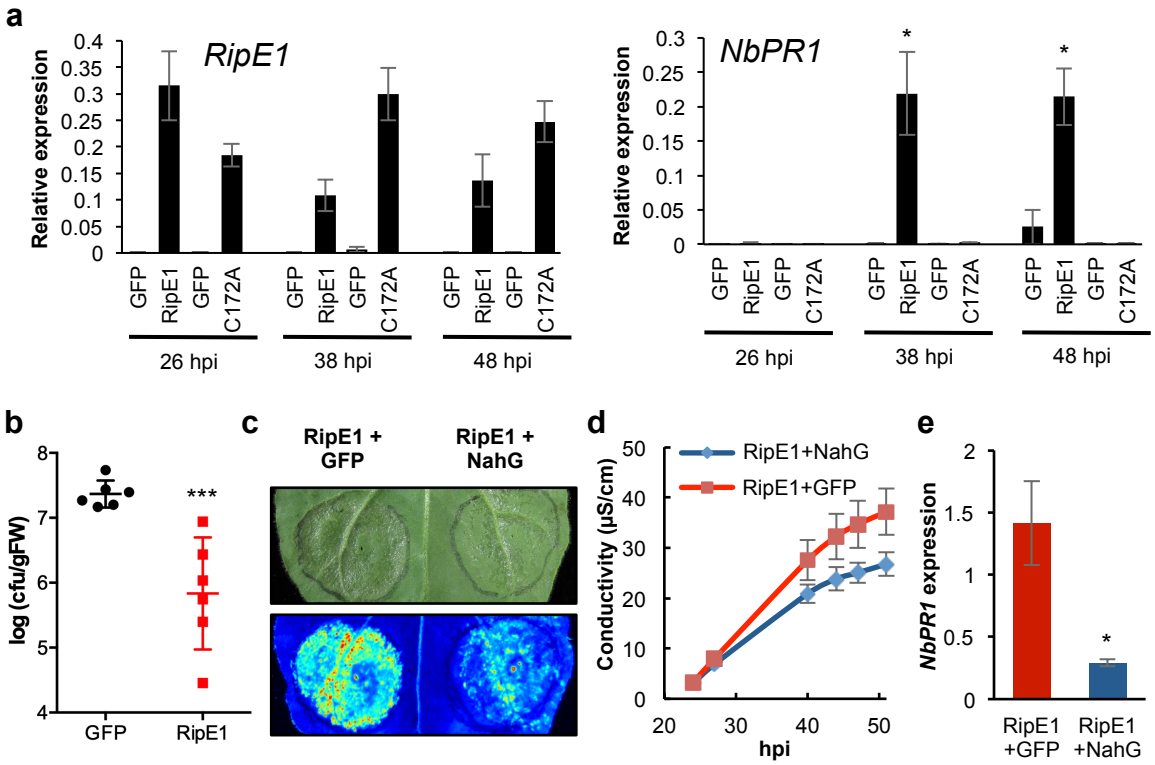

Figure 2. RipE1 activates SA-dependent immune responses in *N. benthamiana*. (a) Quantitative RT-PCR to determine the expression of *RipE1* and *NbPR1* in *N. benthamiana* tissues expressing GFP, RipE1, or RipE1 C172A, using Agrobacterium with an OD_{600} of 0.1. Samples were taken at the indicated times after Agrobacterium infiltration. In each case, the RipE1 variants and their respective GFP control were expressed in the same leaf, and values are represented side-by-side. Expression values are relative to the expression of the housekeeping gene *NbEF1a*. Values indicate mean ± SE (n=3 biological replicates). (b) RipE1-GFP or GFP (as control) were expressed in the same leaf of *N. benthamiana* using Agrobacterium with an OD600 of 0.5. Twenty-four hours after Agrobacterium infiltration, before the appearance of cell death, a 10^5 cfu/ml inoculum of *R. solanacearum* Y45 was infiltrated into the same tissues. Samples were taken one day post-inoculation to determine Y45 colony-forming units (cfu) per gram of tissue. Values indicate mean ± SE (n=6 biological replicates). (c-e) RipE1-Nluc was co-expressed with GFP (as control) or with NahG-GFP in the same leaf. Protein accumulation is shown in the figure S3. (c) Photos were taken 2.5 days post-inoculation with a CCD camera (upper panel) or an UV camera (lower panel). UV signal corresponds to the development of cell death (not GFP fluorescence). UV images were taken from the abaxial side and flipped horizontally for representation. (d) Ion leakage measured in leaf discs taken from *N. benthamiana* tissues expressing RipE1 together with GFP or NahG-GFP, representative of cell death, at the indicated time points. Values indicate mean ± SE (n=3 biological replicates). (e) Quantitative RT-PCR to determine the expression of *NbPR1* in *N. benthamiana* tissues 48 hours after Agrobacterium infiltration. Expression values are relative to the expression of the housekeeping gene *NbEF1a*. Values indicate mean ± SE (n=3 biological replicates). Asterisks indicate significant differences compared to the mock control according to a Student's t test (* $p < 0.05$; *** $p < 0.001$). Each experiment was repeated at least 3 times with similar results.

Figure 3

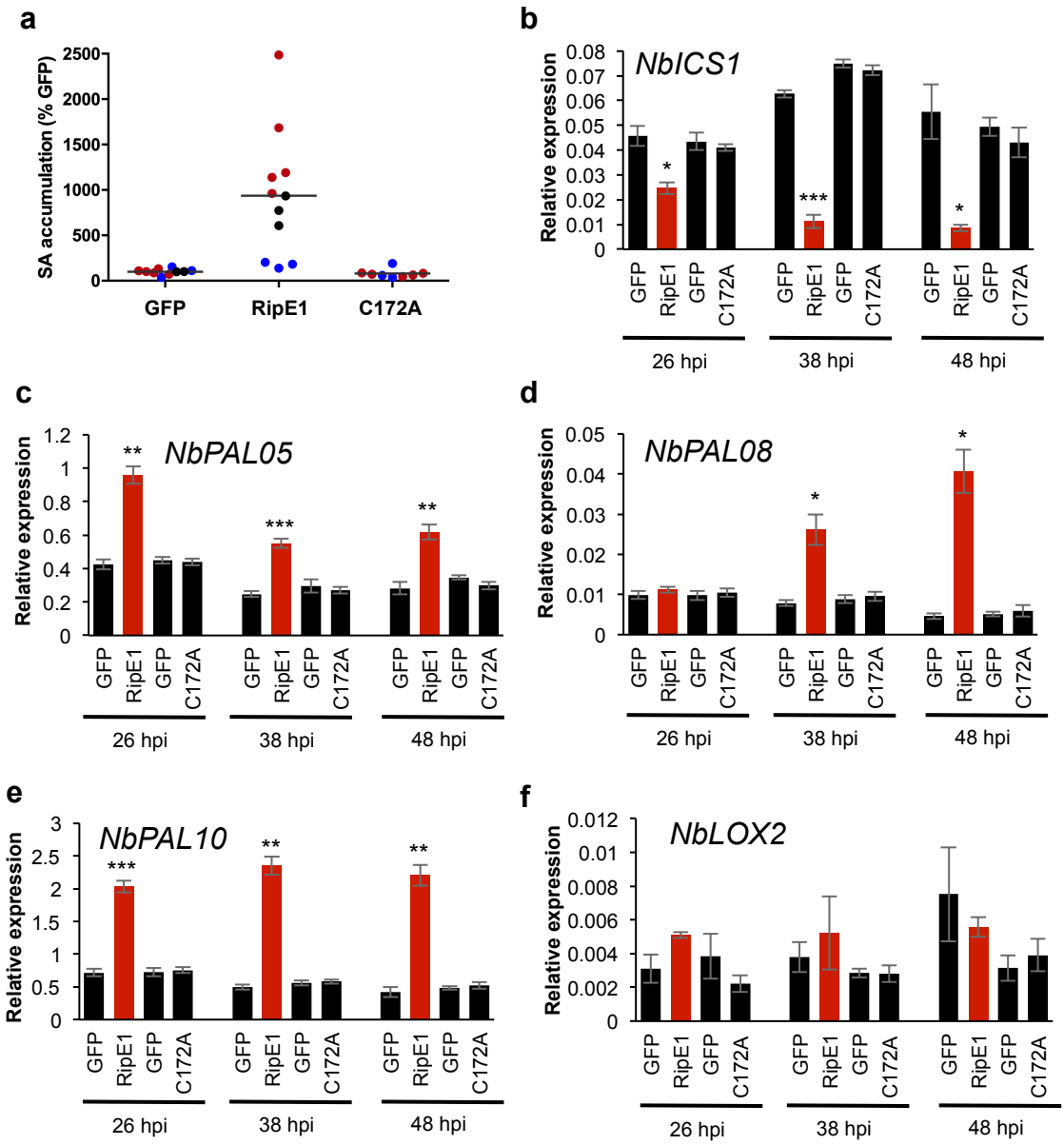

Figure 3. RipE1 perception enhances the expression of *PAL* genes and SA biosynthesis in *N. benthamiana*.

(a) Measurement of SA accumulation in *N. benthamiana* tissues expressing GFP, RipE1, or RipE1 C172A, using Agrobacterium with an OD_{600} of 0.5. Samples were taken 42 hours after Agrobacterium infiltration. Three independent biological repeats were performed, and the different colors indicate values from different replicates. Values are represented as % of the GFP control in each replicate. (b-f) Quantitative RT-PCR to determine the expression of *NbICS1* (b), *NbPAL05* (c), *NbPAL08* (d), *NbPAL10* (e), and *NbLOX2* (f) in *N. benthamiana* tissues expressing GFP, RipE1, or RipE1 C172A, using Agrobacterium with an OD_{600} of 0.1. Samples were taken at the indicated times after Agrobacterium infiltration. In each case, the RipE1 variants and their respective GFP control were expressed in the same leaf, and values are represented side-by-side. *NbPAL05*: Niben101Scf05617g00005.1; *NbPAL08*: Niben101Scf03712g01008.1; *NbPAL10*: Niben101Scf12881g00010.1. Expression values are relative to the expression of the housekeeping gene *NbEF1a*. Values indicate mean ± SE (n=3 biological replicates). Asterisks indicate significant differences compared to the mock control according to a Student's t test (* $p < 0.05$; ** $p < 0.01$; *** $p < 0.001$). Each experiment was repeated at least 3 times with similar results.

Figure 4

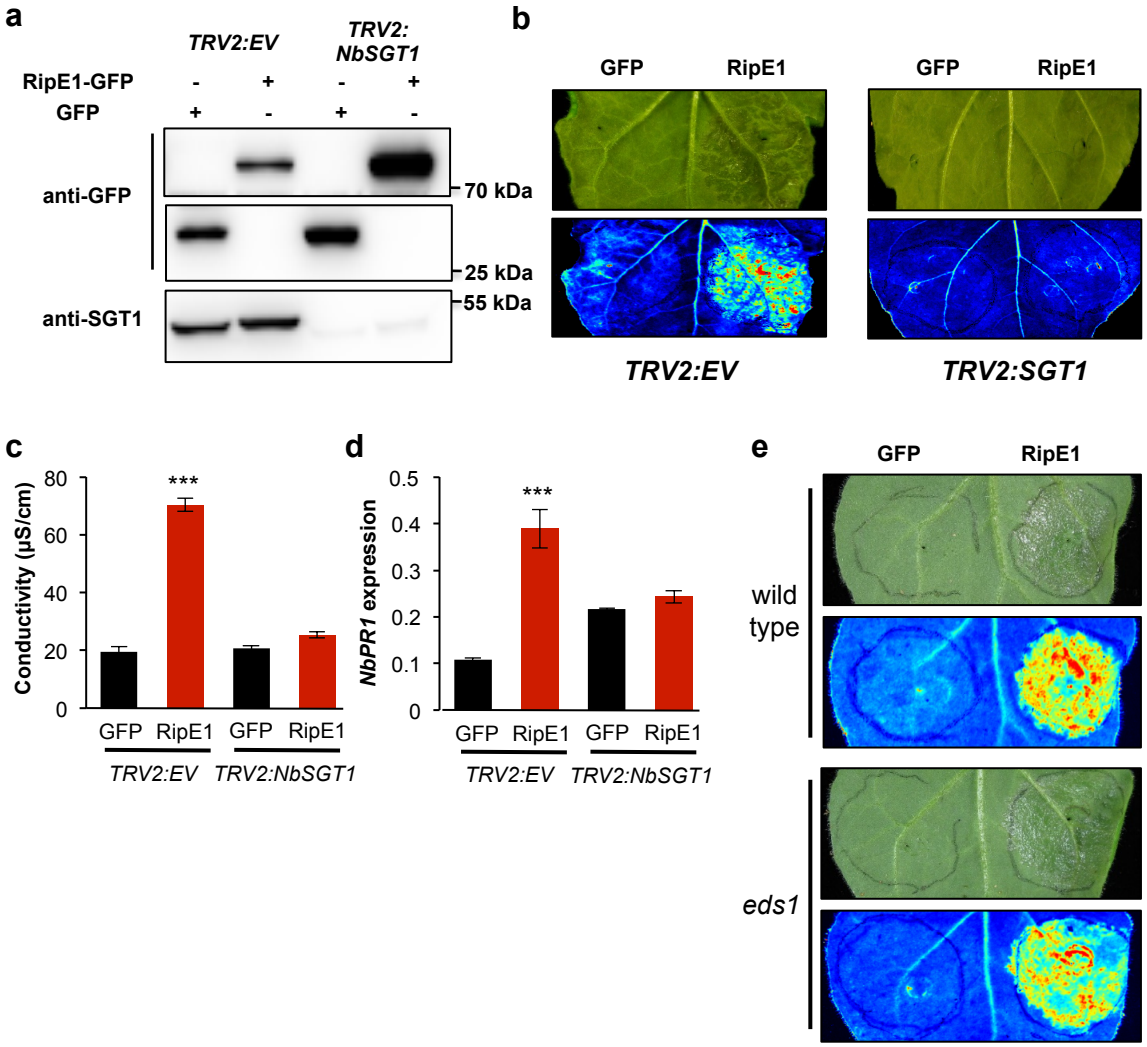

Figure 4. RipE1-triggered responses require SGT1, but not EDS1.
(a-d) RipE1-GFP or GFP (as control) were expressed in the same leaf of *N. benthamiana* undergoing VIGS of *NbSGT1* or VIGS with an empty vector (EV) construct (as control), using Agrobacterium with an OD_{600} of 0.5. (a) Western blot showing the accumulation of GFP, RipE1-GFP, and endogenous *NbSGT1*. Molecular weight (kDa) marker bands are indicated for reference. (b) Photos were taken 2 days post-inoculation with a CCD camera (upper panel) or an UV camera (lower panel). UV signal corresponds to the development of cell death (not GFP fluorescence). UV images were taken from the abaxial side and flipped horizontally for representation. (c) Ion leakage measured in leaf discs taken from *N. benthamiana* tissues expressing RipE1-GFP or GFP (as control), representative of cell death, 48 hours after Agrobacterium infiltration. Values indicate mean ± SE (n=3 biological replicates). (d) Quantitative RT-PCR to determine the expression of *NbPR1* in *N. benthamiana* tissues 48 hours after Agrobacterium infiltration. Expression values are relative to the expression of the housekeeping gene *NbEF1a*. Values indicate mean ± SE (n=3 biological replicates). (e) RipE1-GFP or GFP (as control) were expressed in the same leaf of *N. benthamiana* wild type or a stable *eds1* knockout mutant, using Agrobacterium with an OD_{600} of 0.5. Photos were taken 2 days post-inoculation with a CCD camera (upper panel) or an UV camera (lower panel). UV signal corresponds to the development of cell death (not GFP fluorescence). UV images were taken from the abaxial side and flipped horizontally for representation. Asterisks indicate significant differences compared to the mock control according to a Student's t test (*** $p < 0.001$). Each experiment was repeated at least 3 times with similar results.

Figure 5

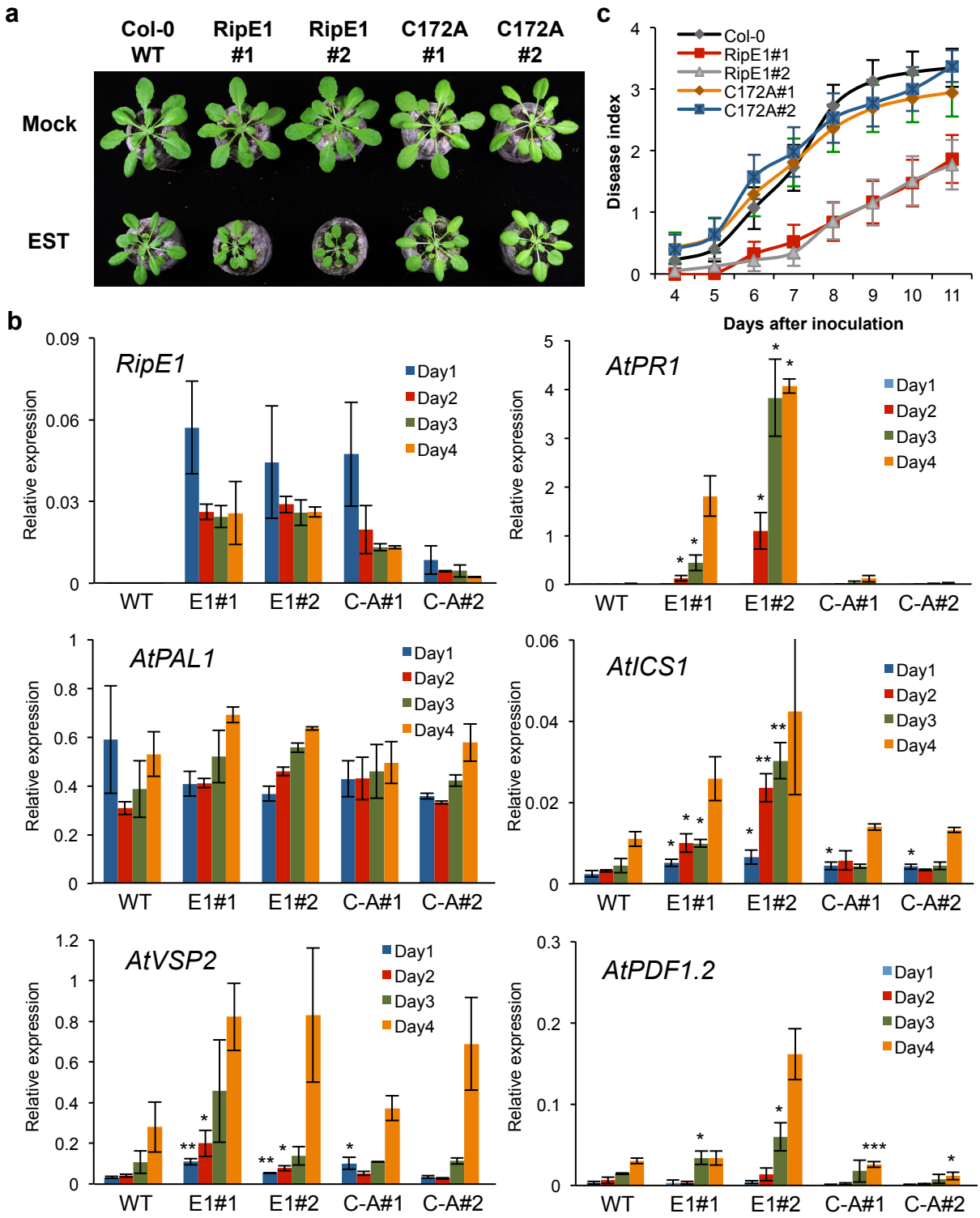

Figure 5. RipE1 triggers immunity in Arabidopsis.
(a) Arabidopsis Col-0 wild type or independent stable transgenic lines expressing RipE1 or RipE1 C172A from an estradiol (EST)-inducible promoter were grown for 3 weeks and then treated sprayed with 100 µM EST daily. Photographs were taken 2 weeks after beginning the EST treatment. (b) Arabidopsis 4 day-old seedlings were treated with 25 µM EST and samples were taken 1, 2, 3, or 4 days after EST treatment. Quantitative RT-PCR to determine the expression of *RipE1, AtPR1, AtPAL1, AtICS1, AtVSP2,* and *AtPDF1.2*. Expression values are relative to the expression of the housekeeping gene *AtACT2*. Values indicate mean ± SE (n=3 biological replicates). (c) Arabidopsis Col-0 wild type or EST-RipE1 transgenic plants were grown for 4 weeks and then treated with 100 µM EST for 2 days before inoculation with *R. solanacearum* GMI1000 by soil-drenching. Plants showed no difference in root or shoot size at the time of inoculation. The results are represented as disease progression, showing the average wilting symptoms in a scale from 0 to 4 (mean ± SEM). n=20 plants per genotype. Asterisks indicate significant differences compared to the mock control according to a Student's t test (* $p < 0.05$; ** $p < 0.01$; *** $p < 0.001$). Each experiment was repeated at least 3 times with similar results.

Figure 6

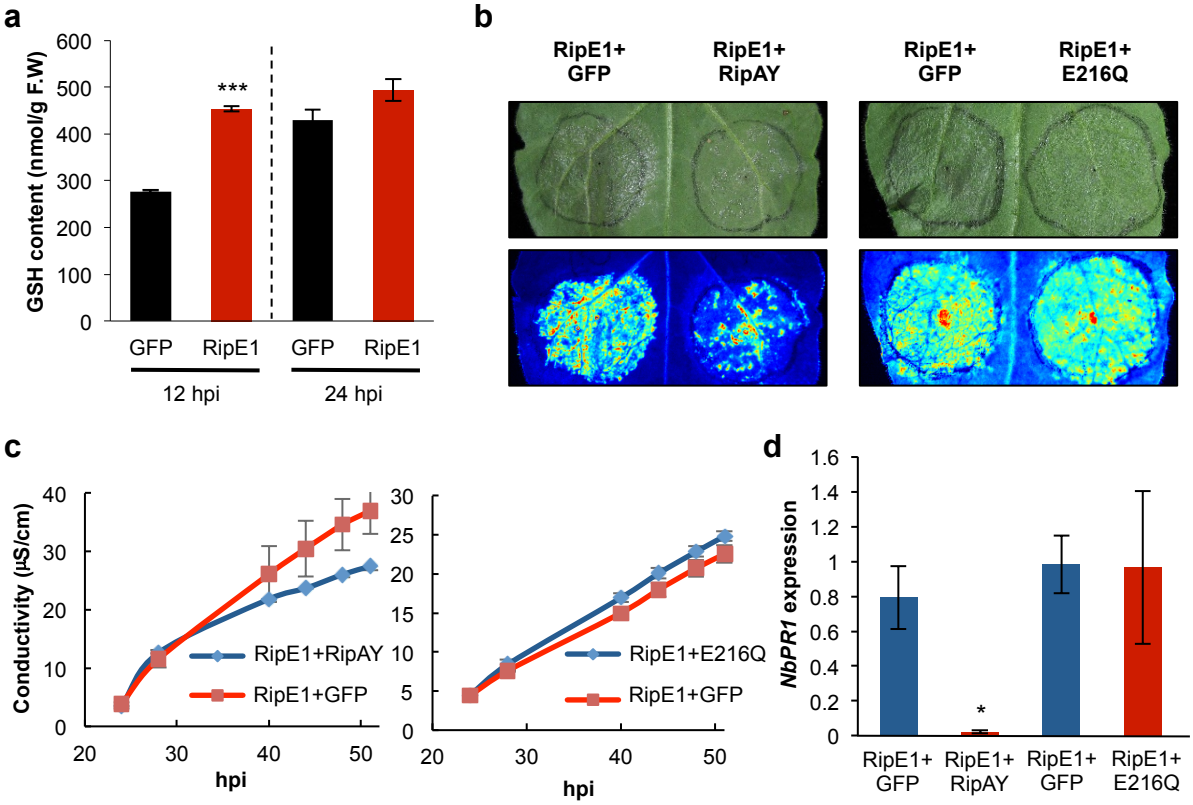

Figure 6. RipE1-triggered immune responses are suppressed by RipAY. (a) RipE1-GFP or GFP (as control) were expressed in the same leaf of *N. benthamiana* using Agrobacterium with an OD_{600} of 0.5, and samples were taken at the indicated time points to measure the accumulation of glutathione (GSH). (b-d) RipE1-Nluc was co-expressed with GFP (as control), with RipAY-GFP, or with RipAY-E216Q-GFP, respectively, in the same leaf. Protein accumulation is shown in the figure S7. (b) Photos were taken 2.5 days post-inoculation with a CCD camera (upper panel) or an UV camera (lower panel). UV signal corresponds to the development of cell death (not GFP fluorescence). UV images were taken from the abaxial side and flipped horizontally for representation. (c) Ion leakage measured in leaf discs taken from *N. benthamiana* tissues expressing RipE1 together with GFP or RipAY-GFP, representative of cell death, at the indicated time points. Values indicate mean ± SE (n=3 biological replicates). (d) Quantitative RT-PCR to determine the expression of *NbPR1* in *N. benthamiana* tissues 48 hours after Agrobacterium infiltration. Expression values are relative to the expression of the housekeeping gene *NbEF1a*. Values indicate mean ± SE (n=3 biological replicates). Asterisks indicate significant differences compared to the mock control according to a Student's t test (* $p < 0.05$; *** $p < 0.001$). Each experiment was repeated at least 3 times with similar results.

Figure S1

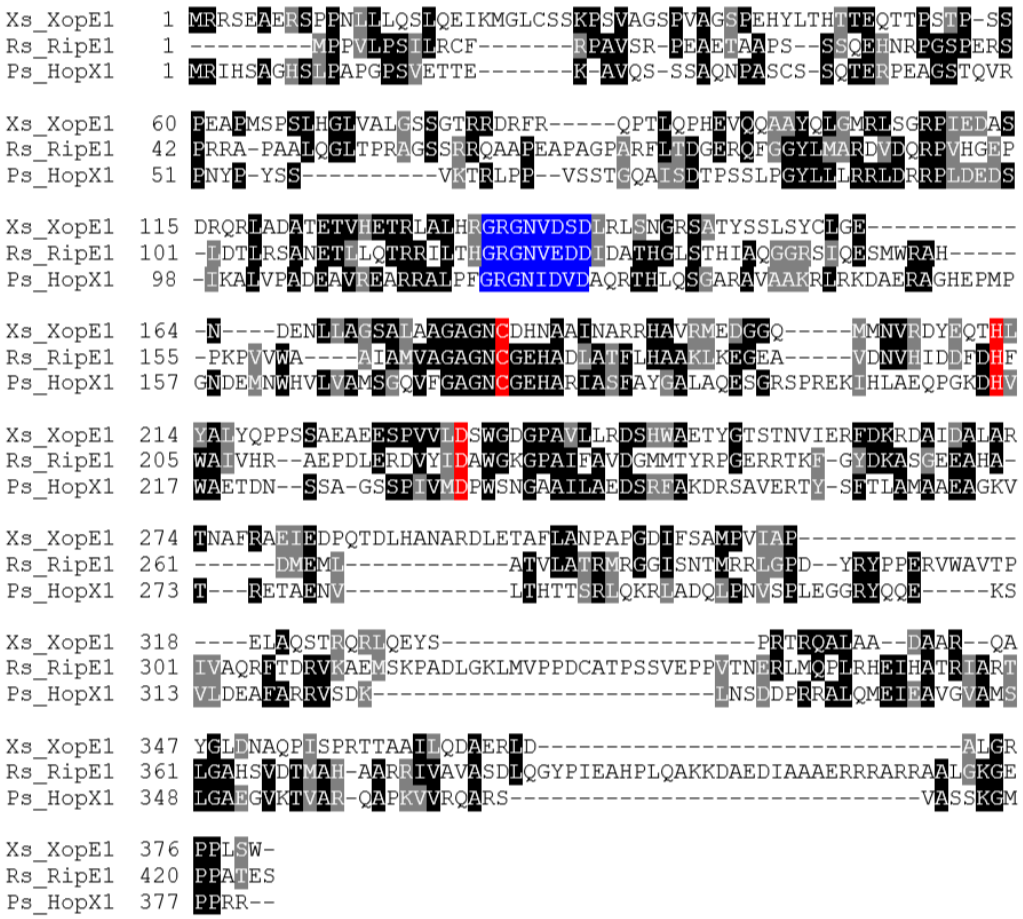

Figure S1. Phylogenetic analysis of RipE1

Alignment of the amino acid sequence of RipE1 from *R. solanacearum* GMI1000 (Rs_RipE1), XopE1 from *Xanthomonas campestris* pv. *vesicatoria* (Xs_XopE1), and HopX1 from *Pseudomonas syringae* pv tabaci 11528 (Ps_HopX1). Residues forming the predicted catalytic triad are indicated in red, and the conserved domain A is indicated in blue. The black shaded amino acids are identical among the three effectors.

Figure S2

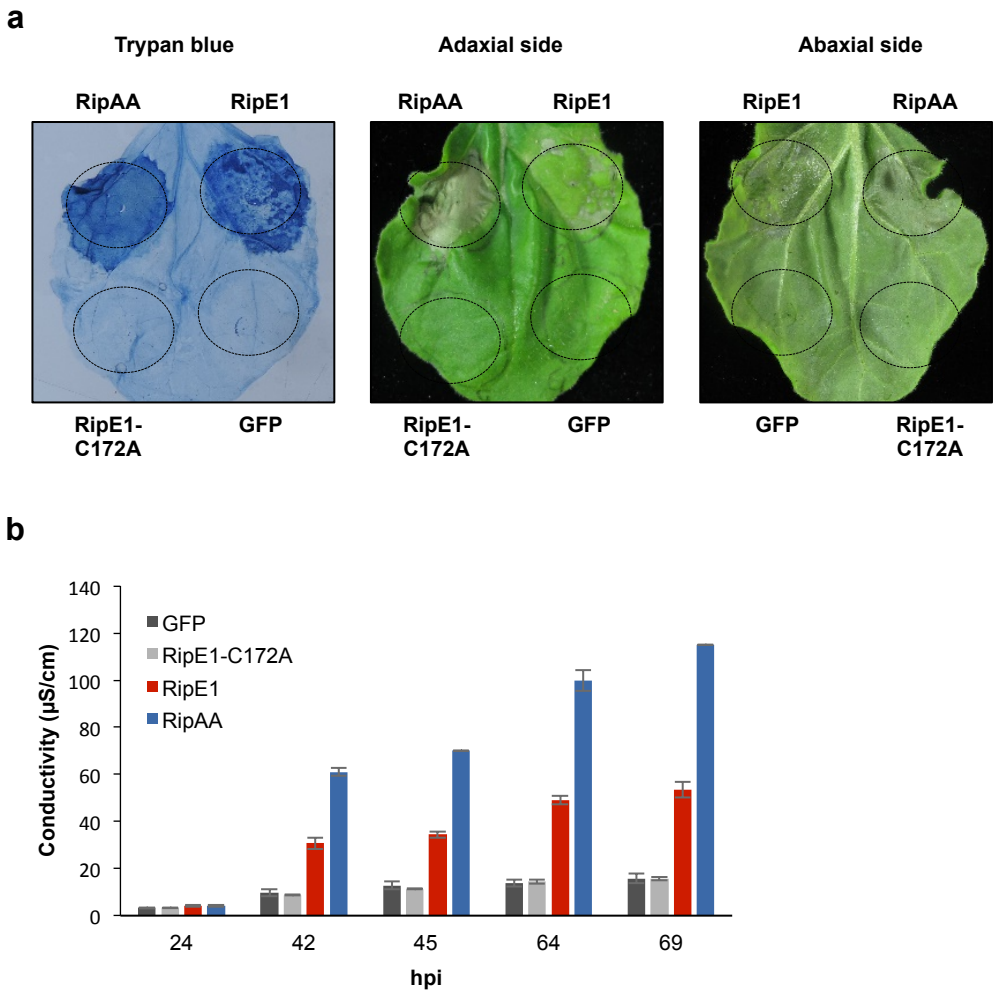

Figure S2. RipE1 induces cell death in *N. benthamiana.*
RipE1-GFP, RipE1-C172A-GFP, RipAA-GFP (as positive control), and GFP (as negative control) were expressed in the same leaf of *N. benthamiana* using Agrobacterium with an OD_{600} of 0.5. (a) Trypan blue staining was performed 4 days post-inoculation, and additional photos of an independent unstained leaf is shown for reference. (b) Ion leakage measured in leaf discs taken from *N. benthamiana* tissues expressing the indicated constructs, at the indicated time points. Values indicate mean ± SE (n=3 biological replicates). These experiments were repeated 3 times with similar results.

Figure S3

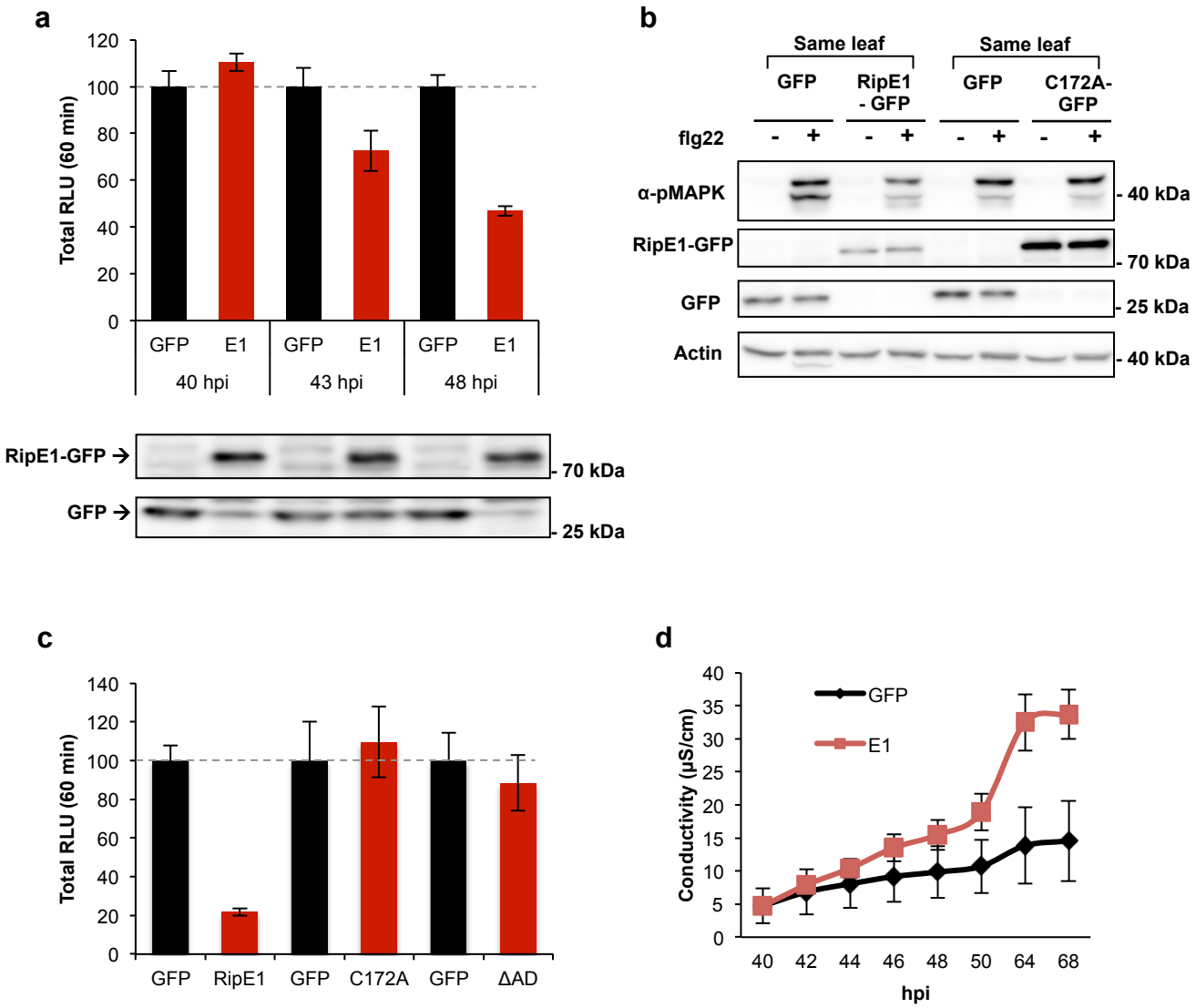

Figure S3. RipE1 expression inhibits PTI responses in *N. benthamiana*, which correlates with the induction of cell death.
Agrobacterium was used to induce the transient expression of RipE1-GFP in half of the leaf and GFP in the other half. (a) Oxidative burst triggered by 50 nM flg22 in *N. benthamiana* tissues at the indicated time points, measured in a luminol-based assay as relative luminescence units (RLU). Values are average ± SE (n=24), and are represented as % of the GFP control in each time point. Western blot with anti-GFP is shown for reference of protein accumulation at each time point. (b) MAPK activation was induced 40 hours after Agrobacterium infiltration with 100 nM flg22 and analysed 15 minutes after flg22 treatment using anti-phosphorylated MAPK antibody (anti-pMAPK). Immunoblots were also analysed using anti-GFP antibody to verify protein accumulation. Anti-actin was used to verify equal loading. Molecular weight (kDa) marker bands are indicated for reference. (c) Oxidative burst was induced as in (a) and measured 2 days post-Agrobacterium infiltration. Mutant variants are described in the Figure 1. (d) Ion leakage was measured as in the Figure 1. Measurement over time after RipE1 expression reflects that the induction of cell death correlates in time with the suppression of PTI responses. The experiments were repeated three times with similar results.

Figure S4

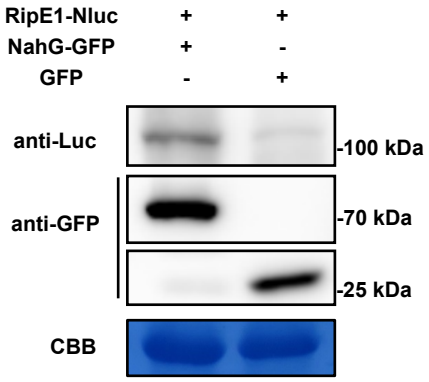

Figure S4. Protein accumulation upon co-expression of RipE1 and NahG.
Western blot showing protein accumulation in the experiments shown in the figure 2. Molecular weight (kDa) marker bands are indicated for reference.

Figure S5

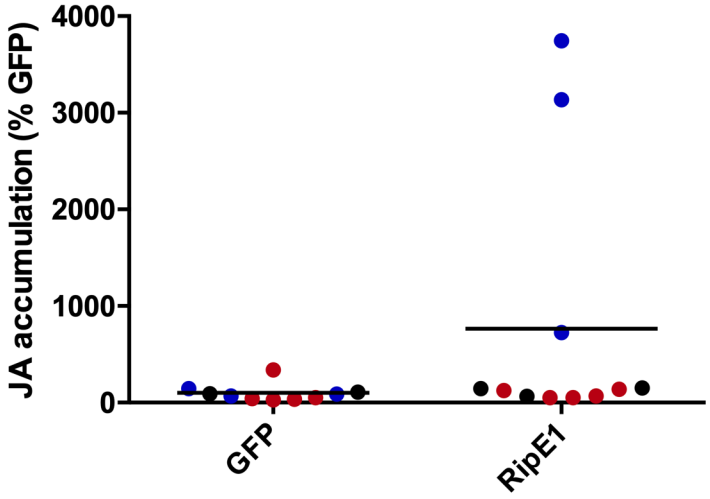

Figure S5. RipE1 expression leads to an increase in JA contents.
Measurement of JA accumulation in *N. benthamiana* tissues expressing GFP or RipE1, using Agrobacterium with an OD_{600} of 0.5. Samples were taken 42 hours after Agrobacterium infiltration. Three independent biological repeats were performed, and the different colors indicate values from different replicates. Values are represented as % of the GFP control in each replicate.

Figure S6

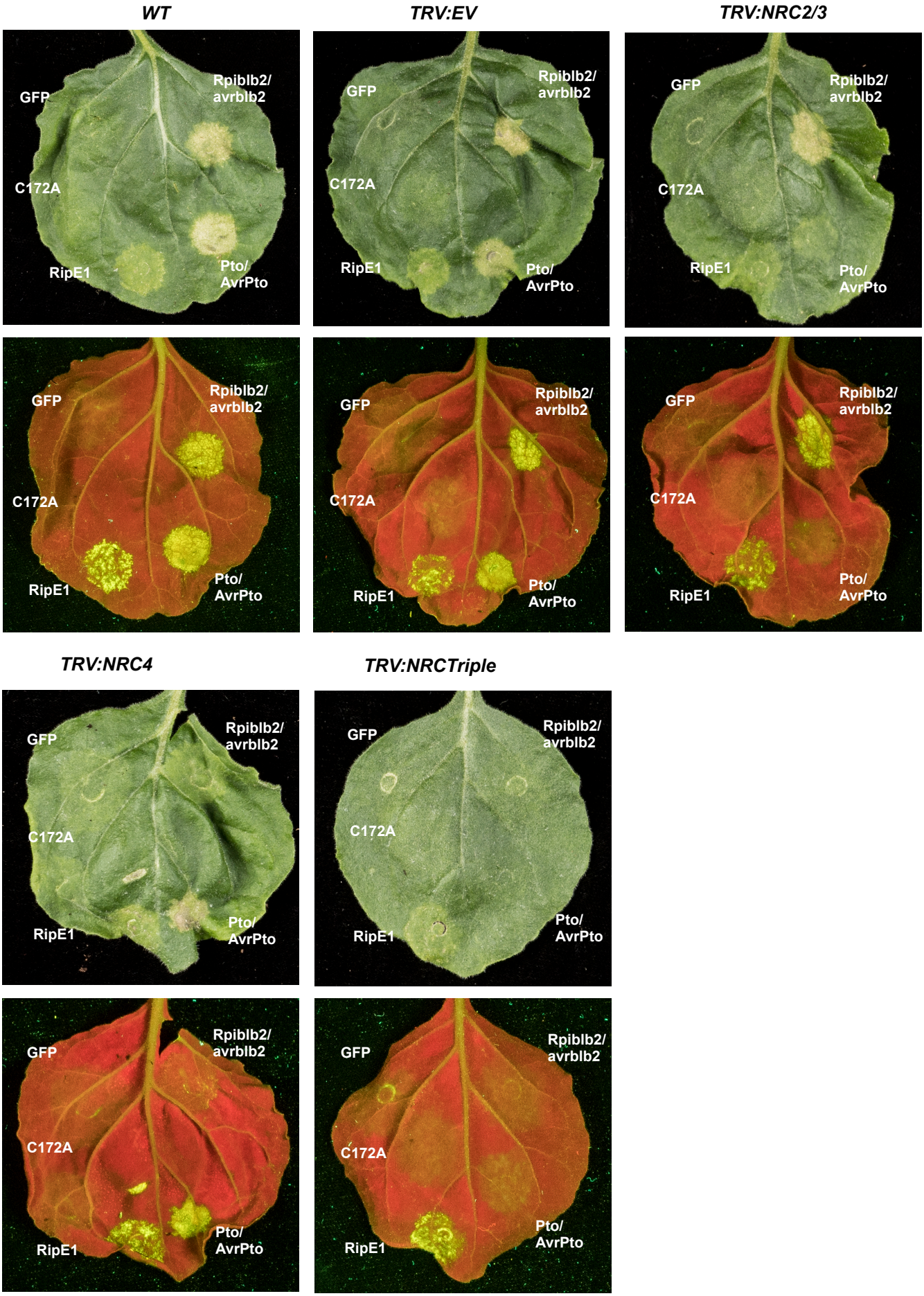
WT
TRV:EV
TRV:NRC2/3
TRV:NRC4
TRV:NRCTriple
GFP
Rpiblb2/
avrblb2
C172A
RipE1
Pto/
AvrPto

Figure S6. RipE1-triggered cell death does not require NRC proteins.
RipE1-GFP, RipE1-C172A-GFP or GFP (as control) were transiently expressed using agrobacterium into wild type (WT) *N. benthamiana*, leaves silenced with EV (as control) and those silenced with different NRC homologs (NRC2/3, NRC4 and NRC2/3/4-Triple), using VIGS. For RipE1-GFP, RipE1-C172A-GFP and GFP an OD_{600} of 0.5 was used. Rpiblb2 (OD_{600} 0.2)/AVRblb2 (OD_{600} 0.1) and Pto (OD_{600} 0.6)/AVRPto (OD_{600} 0.1), which are NRC4 and NRC2/3 dependent, respectively, were included as controls. Photos were taken 5 days post inoculation under natural or UV light. UV images were taken from the abaxial side and flipped horizontally for representation.

Figure S7

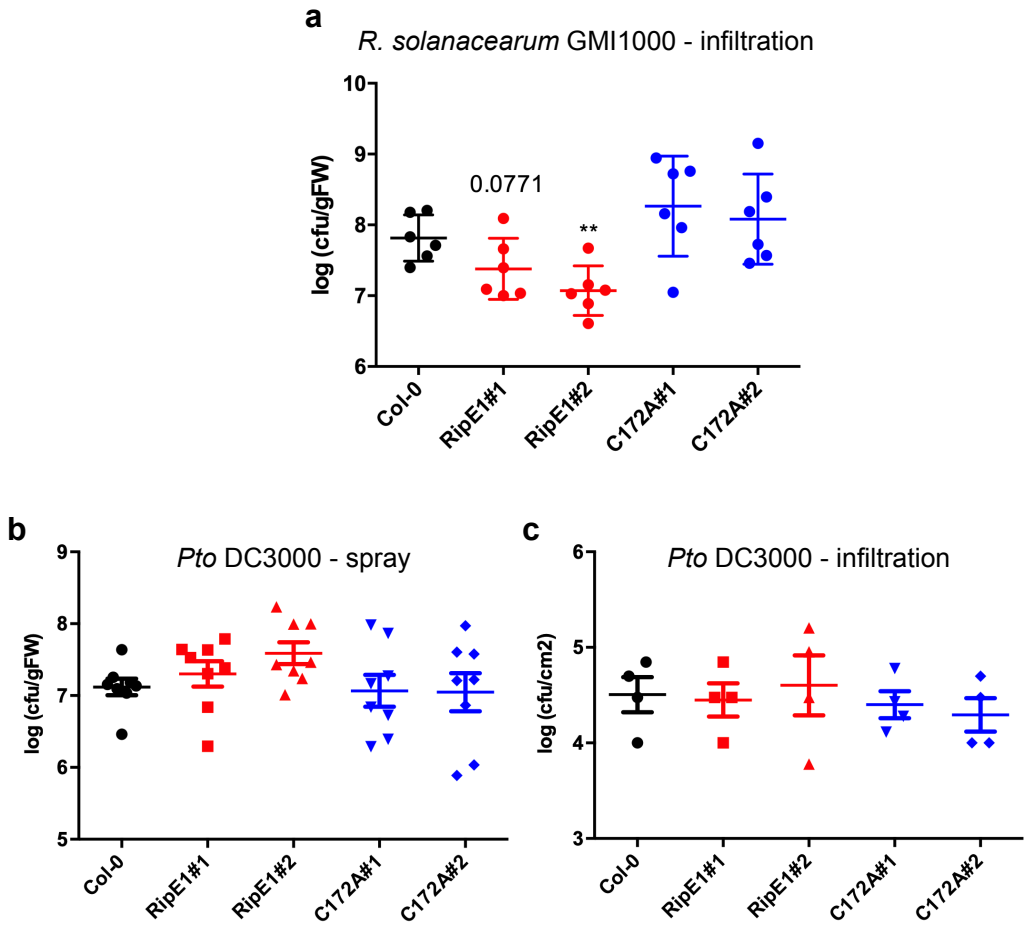

Figure S7. Leaves of RipE1-expressing Arabidopsis plants show enhanced resistance against inoculation with *R. solanacearum*, but not *P. syringae pv tomato* (*Pto*) DC3000.

(a) Growth of *R. solanacearum* GMI1000 (inoculated at 10^7 cfu/ml) infiltrated with a needleless syringe into wild-type Col-0 and RipE1-expressing Arabidopsis plants. Four week-old plants were sprayed with 100 µM estradiol and then covered for 2 days prior inoculation. Bacterial colony-forming units (cfu) were determined 2 days post-inoculation (dpi). Values indicate mean ± SE (n=6 biological replicates). Asterisks indicate significant differences compared to Col-0 WT plants according to a Student's t test (** $p < 0.01$). A specific p value is indicated for the RipE1#1 plant to indicate a reproducible (but not statistically significant) difference in bacterial growth compared to Col-0 WT plants. (b) Growth of surface (spray)-inoculated *Pto* DC3000 (inoculated at 10^8 cfu/ml) in wild-type Col-0 and RipE1-expressing Arabidopsis seedlings. Three week-old seedlings were sprayed with 100 µM estradiol and then covered for 2 days prior inoculation. Bacterial colony-forming units (cfu) were determined 3 days post-inoculation (dpi). Values indicate mean ± SE (n=8 biological replicates). (c) Growth of *Pto* DC3000 (inoculated at 10^5 cfu/ml) infiltrated with a needleless syringe into wild-type Col-0 and RipE1-expressing Arabidopsis plants. Four week-old plants were sprayed with 100 µM estradiol and then covered for 2 days prior inoculation. Bacterial colony-forming units (cfu) were determined 3 days post-inoculation (dpi). Values indicate mean ± SE (n=4 biological replicates). Experiments were repeated more than three times with similar results.

Figure S8

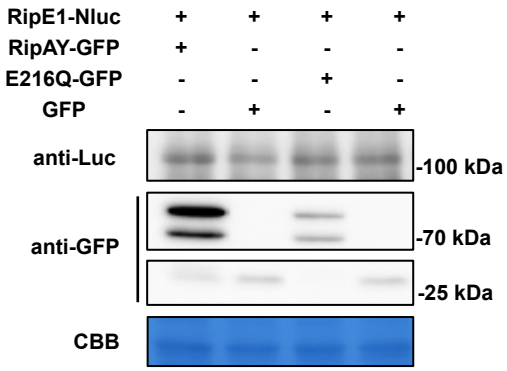

Figure S8. Protein accumulation upon co-expression of RipE1 and RipAY.
Western blot showing protein accumulation in the experiments shown in the figure 6. Molecular weight (kDa) marker bands are indicated for reference.

Figure S9

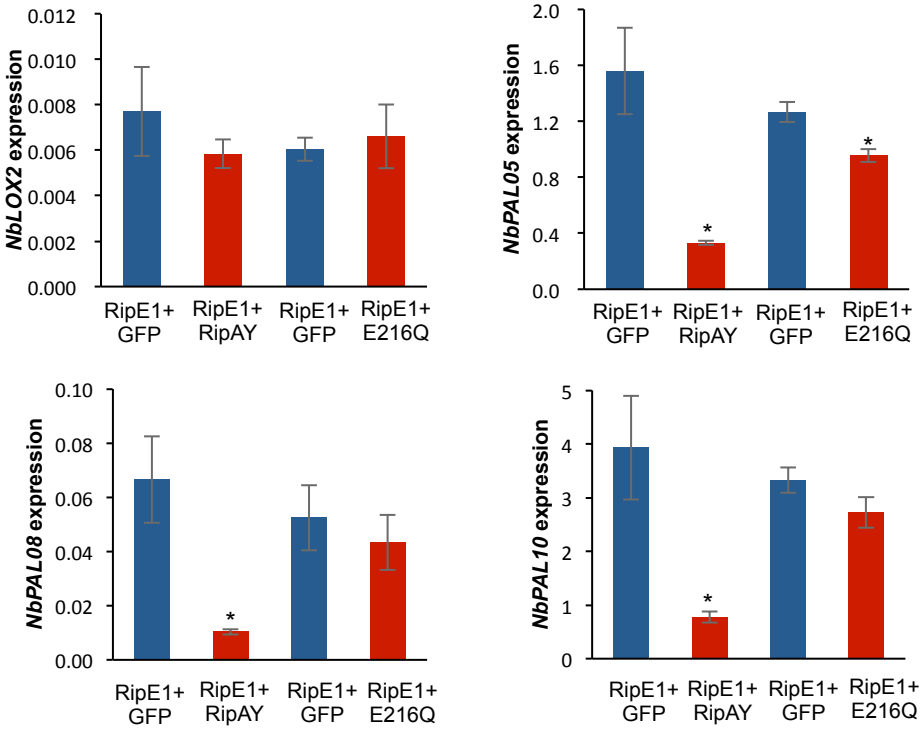

Figure S9. RipAY suppresses the overexpression of SA-related genes triggered by RipE1.
Quantitative RT-PCR to determine the expression of *NbPAL05, NbPAL08, NbPAL10,* and *NbLOX2* in *N. benthamiana* tissues 48 hours after Agrobacterium infiltration. *NbPAL05*: Niben101Scf05617g00005.1; *NbPAL08*: Niben101Scf03712g01008.1; *NbPAL10*: Niben101Scf12881g00010.1. Expression values are relative to the expression of the housekeeping gene *NbEF1a*. Values indicate mean ± SE (n=3 biological replicates). Asterisks indicate significant differences compared to the mock control according to a Student's t test (* $p < 0.05$).